

AIMS Environmental Science

Volume No. 11

Issue No. 1

January - April 2024



ENRICHED PUBLICATIONS PVT. LTD

**S-9, IInd FLOOR, MLU POCKET,
MANISH ABHINAV PLAZA-II, ABOVE FEDERAL BANK,
PLOT NO-5, SECTOR-5, DWARKA, NEW DELHI, INDIA-110075,
PHONE: - + (91)-(11)-47026006**

AIMS Environmental Science

Aims and Scope

AIMS Environmental Science is an international Open Access journal devoted to publishing peer-reviewed, high quality, original papers in the field of Environmental science. We publish the following article types: original research articles, reviews, editorials, letters, and conference reports. All published papers' full text from 2016 will be indexed by WoS.

Aim and scope

AIMS Environmental science is an international Open Access journal devoted to publishing peer-reviewed, high quality, original papers in the field of Environmental science. We publish the following article types: original research articles, reviews, editorials, letters, and conference reports.

AIMS Environmental science welcomes, but not limited to, the papers from the following topics:

- Global climate change & adaption
- Air-water-biota-rock interfaces
- Environmental epidemiology & ecology
- Pollution control & mitigation
- Environmental materials
- Natural resource management
- Waste management
- Geo-hazards
- Environmental risk analysis
- Air & water quality

AIMS Environmental Science

Editor in Chief

Yifeng Wang

Sandia National Laboratories, P.O. Box 5800, Mail Stop 0779,
Albuquerque, New Mexico 87185-0779

Managing Editor

Cheng Bi

Managing and Operation (Journal)

Editorial Board

Juan P. Arrebola	Laboratory of Medical Investigations, San Cecilio University Hospital, University of Granada, 18071-Granada, Spain
Giacomo Assandri	MUSE. Vertebrate Zoology Section Corso del Lavoro e della Scienza 3, I-38123, Trento, Italy
Imad A.M. Ahmed	The University of Lancaster, Lancaster Environment Centre, Lancaster, LA1 4YQ, United Kingdom
Angelo Albini	Dipartimento di Chimica Organica, Università di Pavia, via Taramelli 12, 27100 Pavia, Italy
Mohammednoor Altarawneh	Priority Research Centre for Energy, Faculty of Engineering & Built Environment, The University of Newcastle, Callaghan NSW 2308, Australia
Pasquale Avino	University of Molise, Campobasso, Italy
Alexander Baklanov	Science and Innovation Department, World Meteorological Organization (WMO) 7 bis, Avenue de la Paix, BP2300, CH-1211 Geneva 2, Switzerland
Georgios Bartzas	School of Mining and Metallurgical Engineering, National Technical University of Athens, Greece
Graham S. Begg	The James Hutton Institute, Invergowrie, Dundee DD2 5DA, UK
Cinzia Buratti	Department of Engineering, University of Perugia, Via G. Duranti 63, 06125 Perugia, Italy
Sivaraman (Siv) Balachandran	Department of Chemical and Environmental Engineering, University of Cincinnati, Cincinnati, OH 45221-0012, USA
Carlito B. Tabelin	Laboratory of Mineral Processing & Resources Recycling, Hokkaido University, Sapporo 001-0016, Japan
Andrew R. Barron	Department of Chemistry, Department of Materials Science, Rice University, Houston, Texas 77005, United States
Roberto Bono	Department of Public Health and Pediatrics, University of Torino, ITALY

Michel Boufadel	Department of Civil and Environmental Engineering, New Jersey Institute of Technology 323 MLK Blvd, Newark, NJ 07101 United States (610) 608-2281
Andrea Garcia Bravo	Department of Ecology and Genetics, Limnology, Uppsala University, Norbyvagen 18D, SE-75236 Uppsala, Sweden
Christopher R. Bryant	Geography, University of Montreal, Quebec, Canada and School of Environmental Design, University of Guelph, Ontario, Canada
Carlo Calfapietra	Institute of Agro-Environmental & Forest Biology (IBAF) - National Research Council (CNR), Via Marconi 2, 05010 Porano (TR), Italy
David Carvalho	The Centre for Environment and Marine Studies (CESAM), University of Aveiro, Portugal
Núria Castell	Norwegian Institute for Air Research, P.O. Box 100, NO-2027 Kjeller, Norway
Bing Chen	Northern Region Persistent Organic Pollution Control (NRPOP) Laboratory, Faculty of Engineering & Applied Science, Memorial University of Newfoundland, St. John's, NL A1B 3X5, Canada.
Renato Casagrandi	Dipartimento di Elettronica, Informazione e Bioingegneria (DEIB), Politecnico di Milano (PoliMI), Via Ponzio 34/5, 20133, Milano, Italia.
Hyeok Choi	Department of Civil Engineering, The University of Texas at Arlington, 437 Nedderman Hall, 416 Yates Street Arlington, TX 76019-0308, USA
WONG Man Sing, Charles	Department of Land Surveying and Geo-Informatics, The Hong Kong Polytechnic University
Ian Colbeck	School of Biological Sciences, University of Essex Wivenhoe Park, Colchester CO4 3SQ, UK
Federica Cucchiella	Department of Industrial and Information Engineering and Economics, University of L'Aquila, Via G. Gronchi 18, 67100, L'Aquila, Italy
Fatih Deniz	Department of Environmental Protection Technologies, Bozova Vocational School, Harran University, 63850 Bozova/Sanlıurfa, Turkey
Baolin Deng	Department of Civil and Environmental Engineering, University of Missouri, Columbia, Missouri 65211, USA
Steven D. Warren	USDA, US Forest Service Rocky Mountain Research Station Shrub Sciences Laboratory Provo, UT 84606-1856, USA
Sergi Díez	Department of Environmental Chemistry, Institute of Environmental Assessment and Water Research (IDAEA), Spanish National Research Council (CSIC), C/Jordi Girona, 18-26, E-08034 Barcelona, Spain
Florent Domine	UMI Takuvik, CNRS and Université Laval Pavillon Alexandre Vachon, Université Laval, Québec (Qc) G1V 0A6, Canada

Roy M. Harrison	Division of Environmental Health & Risk Management, School of Geography, Earth & Environmental Sciences, University of Birmingham, Edgbaston, Birmingham B15 2TT, UK
Norman Henderson	Prairie Adaptation Research Collaborative, University of Regina, Regina, Canada
Andrew Hoell	Department of Geography, University of California Santa Barbara, Santa Barbara, CA 93106 (805) 893-8000, USA
Robert W. Howarth	Department of Ecology & Evolutionary Biology, Corson Hall, Cornell University Ithaca, NY 14853 USA
Gordon Huang	Faculty of Engineering and Applied Science, University of Regina, Regina, Sask S4S 0A2, Canada
Nynke Hofstra	Environmental Systems Analysis Group, Wageningen University, P.O. Box 47, 6700 AA Wageningen, the Netherlands
Jeffrey Howard	Dept. of Geology, Wayne State University, 0224 Old Main Bldg. Detroit, MI 48202, USA
Pao Hsiao-Tien	Department of Management Science, National Yang Ming Chiao Tung University, Taiwan
Xiao-Lan Huang	Pegasus Technical Services Inc., 46 E. Hollister Street, Cincinnati, Ohio 45268, USA
Ellard Hunting	Department of Conservation Biology, Institute of Environmental Sciences (CML), Leiden University, Einsteinweg 2, NL-2333 CC, Leiden, The Netherlands
Carlo Ingrao	Department of Economics - University of Foggia; Via Romolo Caggese, 1 - 71121 Foggia, Italy
Ryan Jensen	Department of Geography, Brigham Young University, 622 Spencer W. Kimball Tower, Provo, UT 84602, USA
John Johnston	Ecosystems Research Division, National Exposure Research Laboratory, Office of Research and Development, U.S. Environmental Protection Agency, 960 College Station Road, Athens, Georgia 30605-2700, USA
Rebecca Jordan	Departments of Human Ecology & Ecology, Evolution, and Natural Resources, School of Environmental Biological Sciences, Cook Campus Rutgers, The State University of New Jersey, USA
Çetin KANTAR	Department of Environmental Engineering, Canakkale Onsekiz Mart University, Canakkale, Turkey
Helen M Karlsson	Department of Occupational and Environmental Medicine, Heart Medical Centre, County Council of Ostergotland, Linköping University, 68185 Linköping Sweden
Kasper Kok	Chairgroup Soil Geography and Landcape, Wageningen University & Research Droevendaalsesteeg 3a, 6708 PB Wageningen, the Netherlands

Arunprakash T. Karunanithi	Department of Civil Engineering College of Engineering and Applied Science University of Colorado Denver, 1200 Larimer Street, NC 3027, Campus Box 113, P.O. Box 173364, Denver, CO 80217, USA
Anthony W. King	Environmental Sciences Division, Oak Ridge National Laboratory, P.O. Box 2008, Oak Ridge, TN 37831-6301, USA
Akio Koizumi	Department of Health and Environmental Sciences, Kyoto University Graduate School of Medicine, Kyoto, Japan
Prashant Kumar	Department of Civil and Environmental Engineering, University of Surrey, Guildford GU2 7XH, United Kingdom
He Liu	Department of Environmental Engineering, School of Environmental and Civil Engineering, Jiangnan University, Lihu Avenue 1800, Wuxi, Jiangsu Province, 214122, P. R.China
Yang Liu	Department of Civil and Environmental Engineering, University of Alberta, Edmonton, AB, T6G 2W2, Canada
Marc Levy	Center for International Earth Science Information Network (CIESIN), Earth Institute / Columbia University, 61 Route 9W Palisades, NY 10964, USA
Yuning Li	Department of Chemical Engineering, Department of Chemistry, and Waterloo Institute for Nanotechnology (WIN), University of Waterloo, QNC 5614, 200 University Ave West, Waterloo, Ontario, Canada
Stefano Loppi	Department of Life Sciences, University of Siena Via PA Mattioli 4, I-53100 Siena, Italy
Rafael Luque	Departamento de Química Orgánica, Universidad de Córdoba, Campus de Excelencia Agroalimentario CeIA3, Campus Universitario de Rabanales, Edificio Marie Curie (C3), E-14014 Córdoba, Spain
Piotr Matczak	Affiliation: Institute of Sociology, Adam Mickiewicz University, Szamarzewskiego 89c 60-568 Poznan, Poland
Fabrizio Maturo	University of Campania Luigi Vanvitelli, Caserta, Italy
Paul T. Mativenga	Department of Mechanical, Aerospace & Civil Engineering, School of Engineering, The University of Manchester, Manchester, M13 9PL, United Kingdom
José Miguel Martínez-Paz	Department of Applied Economics., University of Murcia, Campus de Espinardo, 30100 Murcia, Spain
Cristina Menta	Department of Chemistry, Life Sciences and Environmental Sustainability, University of Parma
Justin P. Miller-Schulze	Department of Chemistry, California State University, Sacramento, 6000 J St. Sacramento, CA 95819, USA
Alexandra Monteiro	Department of Economy, Management and Industrial Engineer, University of Aveiro, Aveiro, Portugal

Juan Moreno-Gutiérrez	Departamento de Máquinas y Motores Térmicos, Universidad de Cádiz, Campus Universitario Río San Pedro s/n, 11519 Puerto Real, Spain
Daniel Mueller	Department of Energy and Process Engineering, Norwegian University of Science and Technology, 7491 Trondheim, Norway
Mallikarjuna Nadagouda	US Environmental Protection Agency, National Risk Management Research Laboratory, 26 West Martin Luther King Drive, Cincinnati, OH 45268 USA
Cristina Nerín	Department of Analytical Chemistry, I3A, CPS-University of Zaragoza, María de Luna st. 3, Torres Quevedo Building, E-50018 Zaragoza, Spain
Chukwumerije Okereke	School of Human and Environmental Sciences, University of Reading, Po Box 233, RG6 6AB, UK
Bertram Ostendorf	Spatial Information Group, Earth and Environmental Sciences, University of Adelaide, Glen Osmond, SA 5064, Australia
Gang Pan	Department of Environmental Nanotechnology, Research Center for Eco-environmental Sciences, Chinese Academy of Sciences, 18 Shuangqing Road, Beijing 100085, China
Donguk Park	Department of Environmental Health, Korea National Open University
Alejandro J. Rescia Perazzo	Department of Biodiversity, Ecology and Evolution/Faculty of Biological Sciences, Complutense University of Madrid, Spain
Stefano Pierini	Dipartimento di Scienze e Tecnologie, Università di Napoli Parthenope, Centro Direzionale, Isola C4 - 80143 Napoli, Italy
Oleg S. Pokrovsky	Geoscience and Environment Toulouse, CNRS, Paris, France
Marcelo Francisco Pompelli	Plant Physiology Laboratory, Federal University of Pernambuco, Department of Botany, CCB, Recife, Pernambuco 50670901, Brazil
Albert A Presto	Department of Mechanical Engineering and Center for Atmospheric Particle Studies, Carnegie Mellon University, Pittsburgh, PA 15213, USA
Seeram Ramakrishna	Department of Mechanical Engineering, National University of Singapore, Singapore 117574, Republic of Singapore
Bernhard Rappenglueck	Department of Earth and Atmospheric Sciences (EAS), University of Houston, USA
Jingzheng Ren	The Hong Kong Polytechnic University, Hong Kong SAR, China University of Southern Denmark (Odense, Denmark)
Claire Richard	Institute for Security & Development Policy (Stockholm, Sweden)
	Equipe Photochimie, Clermont Université, Université Blaise Pascal, Institut de Chimie de Clermont-Ferrand (ICCF), BP

Marja-Liisa Riekkola	Department of Chemistry, University of Helsinki, Finland
Martin Leopold	Department Environmental Sciences, University of Helsinki,
Romantschuk	Niemenkatu 73, 15140 Lahti, Finland
David Rojas Rueda	Centre for Research in Environmental Epidemiology (CREAL), Parc de Recerca Biomèdica de Barcelona – PRBB, C. Doctor Aiguader, 88, 08003 Barcelona , Spain
Seena Sahadevan	Marine and Environmental Sciences Centre,,Dept. Life Sciences Faculty of Science and Technology, University of Coimbra P.O. box 3046, 3001-401 Coimbra, Portugal
Dimosthenis Sarigiannis	Department of Chemical Engineering, Aristotle University of Thessaloniki, Greece
Ajit Sarmah	Department of Civil & Environmental Engineering Faculty of Engineering, The University of Auckland, Private Bag 92019, Auckland, New Zealand
Biswajit Sarkar	Department of Industrial Engineering, Yonsei University, South Korea
Marta Schuhmacher	Environmental Engineering Laboratory, Departament d'Enginyeria Quimica, Universitat Rovira i Virgili, Av. Paisos Catalans 26, 43007 Tarragona, Catalonia, Spain
Laura Scrano	Department of European Cultures and Mediterranean (DICEM). University of Basilicata, Potenza – Italy
Jhy-Charm Soo	Health Effects Laboratory Division, National Institute for Occupational Safety and Health (NIOSH), Centers for Disease Control and Prevention, U.S. Department of Health and Human Services (DHHS)
Youngwoo Seo	Department of Civil Engineering, Department of Chemical and Environmental Engineering, University of Toledo, Toledo, Ohio, United States
Jesús Simal-Gándara	Nutrition and Bromatology Group, Analytical and Food Chemistry Department, Faculty of Food Science and Technology, University of Vigo, Ourense Campus, E32004 Ourense, Spain
Carla Patrícia Silva	Department of Chemistry and CESAM, University of Aveiro, Portugal
Karolina M. Siskova	Department of Physical Chemistry, Centre of Advanced Technologies and Materials (RCPTM), Palacky University, Olomouc, CR
Benjamin Sleeter	U.S. Geological Survey - Western Geographic Science Center, 345 Middlefield Road, Menlo Park, CA 94025, USA
Scott Smith	Department of Chemistry Wilfrid Laurier University, 75 University Avenue West, Waterloo, ON, N2L 3C5, CANADA
Christian Sonne	Department of Bioscience, Arctic Research Centre, Aarhus University, Frederiksborgvej 399 P.O. Box 358, DK-4000 Roskilde, Denmark

Sofia Sousa	LEPABE – Laboratory for Process Engineering, Environment, Biotechnology and Energy Chemical Engineering Department Faculty of Engineering, University of Porto, Rua Dr. Roberto Frias s/n, 4200-465 Porto, Portugal
Paul Sutton	Department of Geography and the Environment, 2050 East Iliff Ave, University of Denver, Denver, Colorado 80208, USA
Miklas Scholz	Division of Water Resources Engineering (TVRL), Department of Building and Environmental Technology, Faculty of Engineering, Lund University, P.O. Box 118, 22100 Lund, Sweden
Francesca Ugolini	8, Giovanni Caproni, 50145 Firenze, Italy
Nick Voulvoulis	Centre for Environmental Policy, Imperial College London, London SW7 2AZ, UK
Brigitte Tenhumberg	School of Biological Sciences (SBS) and Department of Mathematics, University of Nebraska-Lincoln (UNL), 412 Manter Hall, Lincoln, NE 68588-0118, USA
Ying I. Tsai	Department of Environmental Engineering and Science, Indoor Air Quality Research and Service Center, Chia Nan University of Pharmacy and Science, 60, Sec. 1, Erren Road, Rende District, Tainan City 71710, Taiwan
Mary Thornbush	Brock University, 500 Glenridge Avenue, St. Catharines, Ontario, L2S 3A1, Canada
Kai Wang	Department of Marine, Earth, and Atmospheric Sciences, North Carolina State University, Campus Box 8208, Raleigh, NC 27695, USA
Shaobin Wang	Department of Chemical Engineering and CRC for Contamination Assessment and Remediation of the Environment (CRC CARE), Curtin University, GPO Box U1987, Perth, WA 6845, Australia
Taoyuan Wei	Center for International Climate and Environmental Research – Oslo (CICERO), P.O. Box 1129 Blindern N-0318 Oslo, Norway
Dominik J Weiss	Department of Earth Science and Engineering, Imperial College London, South Kensington Campus, London SW7 2AZ, UK
J. Michael Wright	U.S. Environmental Protection Agency, National Center for Environmental Assessment, 26 W. Martin Luther King Drive (MS-A110), Cincinnati, OH 45268, USA
Fengchang Wu	State Key Laboratory of Environmental Criteria and Risk Assessment, State Environmental Protection Key Laboratory of Lake Pollution Control, Chinese Research Academy of Environmental Sciences, Beijing 100012, China

Wei Wu

Department of Coastal Sciences, Gulf Coast Research
Laboratory, The University of Southern Mississippi, 703 East
Beach Drive, Ocean Springs, MS 39564 USA

Wei-Min Wu

Department of Civil & Environmental Engineering 473 Via
Ortega, B23, Stanford University, Stanford, CA 94305-4020,
USA

Wassana Yantasee

Department of Biomedical Engineering, OHSU School of
Medicine, Portland, Oregon 97239 USA

Hong Zhang

School of Engineering and Built Environment, Griffith
University, Australia

Jia-Zhong Zhang

Ocean Chemistry Division, Atlantic Oceanographic and
Meteorological Laboratory, 4301 Rickenbacker Causeway,
Miami, Florida 33149, USA

Jiping Zhu

Exposure and Biomonitoring Division, Health Canada,
Ottawa, Ontario, Canada

AIMS Environmental Science

(Volume No. 11 Issue No. 1 January - April 2024)

Contents

Sr. No	Articles/Authors	Pg No
01	Bias of automatic weather parameter measurement in monsoon area, a case study in Makassar Coast <i>- Nurtiti Sunusi¹, and Giarno²</i>	1 - 14
02	A Study of Infaunal Abundance, Diversity and Distribution in Chettuva Mangrove, Kerala, India <i>- Rukhsana Kokkadan¹, Resha Neznin¹, Praseeja Cheruparambath², Jerisa Cabilao¹ and Salma Albouchi</i>	15 - 24
03	Radioactive waste management and disposal – introduction to the special issue <i>- María Sancho</i>	25 - 27
04	Evaluation of river water quality in a tropical South Sumatra wetland during COVID-19 pandemic period <i>-Muhammad Rendana¹, Yandriani¹, Muhammad Izzudin², Mona Lestari³, Muhammad Ilham Fattullah¹ and Jimmy Aldian Maulana¹</i>	28 - 40
05	Soil erosion estimation using Erosion Potential Method in the Vjosa River Basin, Albania <i>-Olton Marko¹, Joana Gjipalaj¹, *, Dritan Profka¹ and Neritan Shkodrani²,</i>	41 - 53

Bias of automatic weather parameter measurement in monsoon area, a case study in Makassar Coast

Nurtiti Sunusi^{1,*} and Giarno²

¹ Department of Statistics, Faculty of Mathematics and Natural Sciences,
Hasanuddin University, Makassar 90245, Indonesia

² State College of Meteorology Climatology and Geophysics, Tangerang 15221,
Indonesia

ABSTRACT

The shift from manual weather measurements to automation is almost inevitable. When switching to AWS (Automatic Weather Station), WMO requires parallel data testing between automatic and manual measurements to be performed. The purpose of this paper is to conduct a parallel test of AWS data using a simple statistical test that has been applied to three main weather parameters, namely temperature, pressure, humidity, rainfall, and wind direction and speed. The months of January and June were used as samples to represent the character of the wet and dry seasons in the Makassar monsoon area. The results of the analysis show that during the rainy season, only pressure and temperature are identical and homogeneous. Meanwhile, in the dry season, apart from these two parameters, humidity and wind speed are also homogeneous and rainfall is a non-homogeneous parameter in January and June. Both AWS and manual observations show that the influence of landsea winds in Makassar is very strong. Considering that there are inhomogeneous parameters, it is highly recommended to test for a longer time, taking into account the season, the influence of other global phenomena, the effect of missing data and incorrect data testing various methods of homogeneity and characteristics in each place and their effect on forecasts.

Keywords: *accuration; bias; Makassar; automatic; manual; weather observation*

1. Introduction

Since 2014, Badan Meteorologi Klimatologi dan Geofisika (BMKG) or the Indonesian Meteorology, Climatology and Geophysics Agency has determined that it will switch weather observations from manual to automatic in the entire BMKG weather observation network. One of the obstacles to improving the quality of data spatially and temporally is the limited capacity of human resources (untrained) and the difficulty of reaching certain locations [1,2]. Automation is one solution to improve the quality and quantity of BMKG observation data, both spatially and temporally. This modernization is very important to keep up with the digital era as well as to increase the quantity and quality of weather data so as to produce fast, precise, and accurate meteorological, climatological and geophysical information which is the current vision of the BMKG [3]. The problem that arises from the transition from manual to automatic weather observations is the suitability of the automatic observation data and the previous manual data [4]. This alignment effort requires parallel testing of these two data types. Meteorological observations manually (OBS) in the BMKG environment are generally obtained with standards, such as measuring instruments, observation method, time of observation, reporting, location, and equipment park [5]. But as technology advances, many things become recorded, digitized, and automated. Even in the 2020 era, there are demands for memorization, which inevitably BMKG also has to adjust.

The term automatic weather observation according to the World Meteorological Organization (WMO)

is weather observations obtained from weather equipment that can record and transmit data automatically [6]. This collection of equipment that measures several weather parameters is known as an automatic weather station. In contrast to manual weather observations, which are weather observations using a tool whose observations are recorded manually. One way to maintain the quality of observational data is to conduct measurement alignment automatically and manually within a minimum period of a year or two years and check for differences [7]. However, the WMO suggests that it is necessary to parallelize automatic weather observations over a certain period [8]. This process requires data from AWS to meet quality control (QC) requirements with statistical methods. The results of this quality control are very important in producing realistic and validated data that can be used as a basis for claiming that the data on the spot is a continuation of the previous manual observation.

A comparison of automatic and manual data in China found that there were variations in rainfall and air temperature, although they were still within tolerable limits [9]. However, this difference could be caused by a change in the tools used [10] or the data is not homogeneous [11]. The difference between these two types of measurement may be quite significant in the long run [12]. According to the research report in the Indonesian region, it shows that bias occurs during extreme conditions [13]. The difference between these two measurements is also influenced by location, where these two types of data are not normally distributed and are not homogeneous [14].

The coastal area which is the border of the sea and land is influenced by diurnal circulation in the form of sea breezes and land breezes. Likewise, Makassar City, which borders the Makassar Strait and the Java Sea, is significantly influenced by monsoon circulation and local wind circulation on land and sea [15]. The monsoon cycle can be seen from the nature of the rain that changes every half year, while the presence of land-sea winds can be detected by the dominant changes in westerly and southeasterly winds almost throughout the year in this city. If the estimation of rainfall using satellites that are very far away is quite good in this place compared to other places in South Sulawesi, are the measurements using AWS also less different than manual data [16–18]. Considering that weather observations will be transferred automatically and most of Indonesia's population is located in coastal areas, this change should not reduce the accuracy of meteorological data. Parallel comparison between these two measurements becomes very important to do. Therefore, the purpose of this study is to calculate and analyze the parallel measurement bias between manual parameter observations and automatic measurement data in coastal areas with monsoon patterns.

2. Materials and methods

2.1. Data and location

This study uses weather observation data in Makassar City, to be precise at the Paotere maritime meteorology station. As a city that has a strategic position because it is at the crossroads of trade traffic lanes, Makassar is a city that is developing very rapidly both in terms of economy and population dynamics. Makassar City is located at coordinates 1190BT and 5.80LS with an elevation of 1–32 meters above sea level. This tropical city is always warm all year round with air temperatures ranging from 20 °C to 39 °C. The weather observation location is located in Paotere, which is the heritage port of the Gowa Sultanate—Tallo Perahu which is located in Ujung Tanah District, Makassar, South Sulawesi. This port is ± 5 km from Makassar City Square (Karebosi Field). Paotere is one of the most historic heritage folk harbors that still survives and is a testament to the legacy of the Gowa-Tallo Sultanate since the XIV century, where the 2nd King of Tallo Karaeng Same ri Liukang once dispatched 200 Phinisi Boat fleets to Malacca. Currently, Paotere Harbor is still normally used as a place for people's boats to dock, such as the phinisi and lambo. This place is also a trading center for fisherman's

catch, which can be seen along the road in the harbor lined with shops selling various types of dried fish, and fishing equipment, as well as several seafood restaurants. According to Baharuddin, who works as a supervisor at Paotere Harbor, the word Paotere comes from the word Otere, which is a rope used in ships that dock. The location of the AWS equipment and manuals is near the Paotere fish auction as shown in Figure 1. Recorded in the last 10 years, the maximum annual rainfall reached 3693 mm in 2017 and the highest rainfall intensity in an hour reached 110 mm on December 16, 2014.

The location of manual observation equipment is in the world standard meteorological instrument park [15]. Manual equipment consists of various types, for example a digital barometer which is recorded every hour by the brand Vaisala, a digital anemometer produced by RM Young 26800, a manual rainfall meter which is measured every 3 hours and air temperature using a Schneider mercury thermometer. While, automatic weather station is produced by Vaisala and is located close to the Makassar Strait waters than the tool park. Unlike the manual rain gauge, the AWS rain gauge is a tipping bucket type with a sensitivity of 0.5 mm. The distance of the automatic weather system to the meteorology cage in the tool park is about 10 meters as shown in Figure 1. The anemometer elevations of these two types of tools are the same height, which is about 10 meters, while the temperature and humidity sensors are 50 cm apart. The data used in this study is data on all-weather parameters obtained by both types of observations. Humidity, air pressure, average, minimum, and maximum temperature, rainfall and wind direction and speed. January was chosen to represent the difference between observations using AWS and manual when there was a lot of rain, while June was to represent the dry season. The temporal resolution of AWS is very high, where data can be degenerated in 10 minutes, while the highest manual observation data can only be every hour. Both types of observations use the world standard time of the UTC universal time coordinate so that comparisons can be made directly.

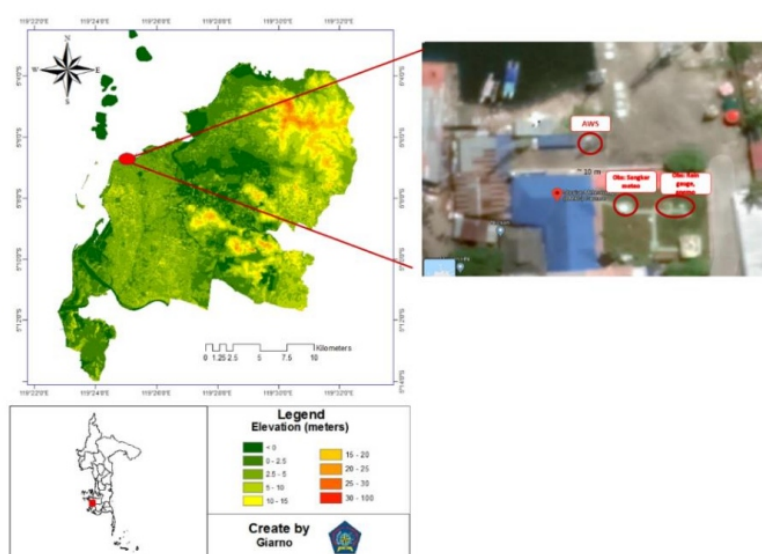


Figure 1. Location of AWS and manual weather observation equipment at Stamar Paotere Makassar.

2.2. Methods

In general, automatic and manual measurements of weather data generally have an abnormal distribution, but the homogeneity test generally shows that both are homogeneous [14,19–22]. The value of the difference between these two measurements is visible when using the calculation of the root mean square error, and correlation [13,23–25]. The difference between automatic and manual measurements in this study uses six methods, namely homogeneity analysis, statistical comparison of

values and visually using wind rose for wind direction. The wind variable is a vector quantity that is very difficult to distinguish using only numbers. Visualization in this research uses wind rose because it is easy to analyze and can describe the distribution of wind distribution very clearly. Meanwhile, to calculate the difference between automatic and manual measurement results, correlation, root mean square error (RMSE), and mean absolute error (MAE) were formulated using Eqs (1)–(3).

$$r = \frac{\sum_{i=1}^N (O_i - \bar{O})(M_i - \bar{M})}{\sqrt{\sum_{i=1}^N (O_i - \bar{O})^2} \sqrt{\sum_{i=1}^N (M_i - \bar{M})^2}}, \quad (1)$$

$$RMSE = \frac{\sqrt{\sum_{i=1}^N (M_i - O_i)^2}}{N}, \quad (2)$$

$$MAE = \frac{\sum_{i=1}^N |M_i - O_i|}{N}, \quad (3)$$

where N is the number of observations, O is the value of the weather parameter in the automatic tool, M is the value of the weather parameter in the manual, \bar{O} is the average value of the weather parameter in the automatic tool, \bar{M} is the average value of the weather parameter in the manual.

Correlation (r) measures the strength and direction of the relationship between variables [26]. The correlation value ranges between –1 and 1, where a value of 1 indicates a strong relationship between variables and is considered to have no relationship if the correlation is 0. A positive sign indicates a change in the direction of the variable in the same direction, while a negative sign indicates a change in the opposite direction. Much of the literature on correlation statistics is divided into 5 classes, namely uncorrelated (0.00–0.20), weak (0.21–0.40), moderate (0.41–0.60), strong (0.61–0.80) and very strong if the value is > 0.80. Karaseva et al. and Prasetya et al. divide the correlation, which is strongly correlated if the value of $r \geq 0.50$ [1,27]. Although there are also many evaluations of remote sensing rainfall estimates, the category of strong and weak correlation is not stated [28–32].

RMSE and MAE values are measures of deviation between automatic and manual tools. If each deviation is added up and divided by the amount of data, then the average size of the deviation is obtained. But the direct addition will cause each other to cancel the value of the deviation if there are positive and negative values. In contrast to the use of absolute values which will reduce the nature of mutually canceling deviations. This calculation is known as the mean absolute error or MAE. The weakness of the negating nature of the number of deviations can also be eliminated using the root mean square error or RMSE because each deviation is squared which automatically results are all positive. It's just that RMSE is sensitive to the value of outliers or outliers [31]. In contrast to the homogeneity test, which is a test of whether or not the variances of two or more distributions are equal. The homogeneity test that will be discussed in this paper is the homogeneity test of variance. The statistical homogeneity test was carried out to determine whether the data in the automatic weather variable O and manual M were homogeneous or not using varied data [33]. Equation (4) is the variance formulation which is applied to the results of manual and automatic observations.

$$Var_O = \sqrt{\frac{\sum_{i=1}^N (O_i - \bar{O})^2}{n(n-1)}}, \quad (4)$$

$$Var_M = \sqrt{\frac{\sum_{i=1}^N (M_i - \bar{M})^2}{n(n-1)}}.$$

To test for homogeneity, the F test was used.

$$F = \frac{Var_o}{Var_M}. \quad (5)$$

The F value is obtained from Fisher's statistical table. Equation (5) is used if the automatic variance is greater than the manual one. If the opposite happens, Eq (5) must be reversed with the automatic variance as a divisor, so that the result is that the F value is always greater than or equal to 1. While the test hypothesis $H_0: Var_o = Var_M$, $H_1: Var_o \neq Var_M$.

Besides statistical calculations and homogeneity tests, wind rose diagrams are also used. This is because the direction variable cannot be directly tested using numerical calculations.

3. Results

Based on the homogeneity test, it was found that not always these two types of measurements are homogeneous. The amount of rainfall and its value greatly affect the homogeneity of AWS measurements and manual observations. In January only the results of temperature and pressure measurements were homogeneous as can be seen in Table 1. The F test values for wind speed, humidity and rainfall were greater than the F table values, which means that the AWS and manual data for these parameters were not homogeneous.

Different results were obtained from the calculation in June 2020, where in this month the rainfall was very rare. Based on the homogeneity test, only rainfall that is not homogeneous from the two types of measurements is obtained. The least amount of rainfall affects the homogeneity of AWS measurements and manual observations. This month only the results of rainfall measurements are not homogeneous as can be seen in Table 2. The F test values for wind speed, humidity and rainfall parameters are smaller than the F table values, which means that AWS and manual data for these parameters are homogeneous. The statistical comparison between AWS and manual using Correlation, RMSE and MAE in January and June can be seen in Tables 3 and 4. Except for rainfall, the correlation between the two types of data is generally strong to very strong. Measurements of temperature, pressure, and humidity are very strong with a correlation of more than 0.9, in contrast to wind speeds of only 0.76 to 0.81. While the rainfall in the two measurements is very weak correlation. AWS and manual deviations for temperature, wind speed and rainfall bias values are higher during the rainy season compared to when there is no or infrequent rain. Meanwhile, at the same time, the pressure and humidity values are usually higher during the dry season.

Table 1. Homogeneity test January 2020.

Parameter	Temperature	Pressure	Speed wind	Humidity	Rainfall
Variance-AWS	5.660	2.699	12.876	75.470	27.213
Variance-OBS	5.914	2.675	9.133	66.170	73.364
F _{count}	1.045	1.009	1.410	1.141	2.696
F _{Tabel}	1.128	1.128	1.128	1.128	1.233
Decision	Homogeneous	Homogeneous	Non-homogeneous	Non-homogeneous	Non-homogeneous

Table 2. Homogeneity test June 2020.

Parameter	Temperature	Pressure	Speed wind	Humidity	Rainfall
Variance-AWS	5.131	1.581	4.101	95.616	0.192
Variance-OBS	5.189	1.561	3.544	96.718	0.320
F _{count}	1.011	1.013	1.157	1.011	1.664
F _{Table}	1.131	1.131	1.365	1.131	1.237
Decision	Homogeneous	Homogeneous	Homogeneous	Homogeneous	Non-homogeneous

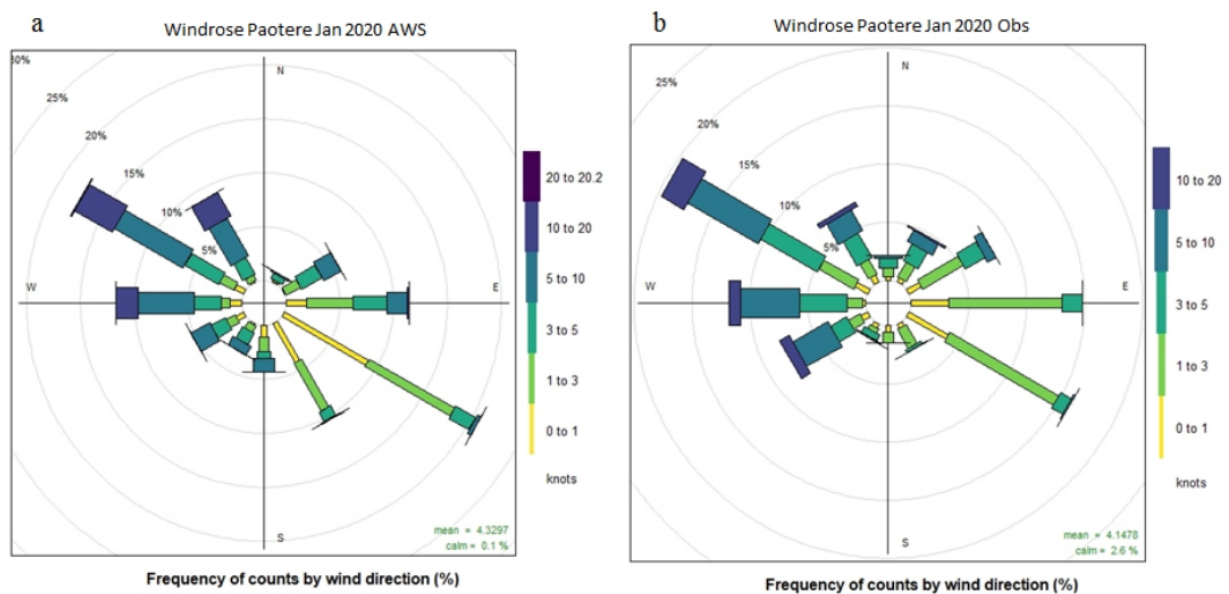
Table 3. Correlation statistics of correlation, RMSE, and MAE January 2020.

Parameter	Temperature	Pressure	Speed wind	Humidity	Rainfall
Correlation	0.970	0.980	0.810	0.940	-0.100
RMSE	1.430	0.340	2.090	3.430	10.560
MAE	-1.320	0.000	0.180	1.590	-1.590

Table 4. Correlation statistics, RMSE and MAE June 2020.

Parameter	Temperature	Pressure	Speed wind	Humidity	Rainfall
Correlation	0.970	0.970	0.760	0.920	0.900
RMSE	1.540	0.370	1.410	4.400	0.250
MAE	-1.450	0.180	-0.340	2.080	-0.010

The homogeneity test resulted in significant differences in wind and humidity values from January and June, both of which were not homogeneous in January and became homogeneous in June. In the wind, in addition to the wind speed component, there is a wind direction component that should be a comparison. The comparison of the wind and its direction is carried out using wind rose as shown in Figure 2 for January and Figure 3 for June.

**Figure 2.** Windrose AWS (a) and manual (b) January 2020.

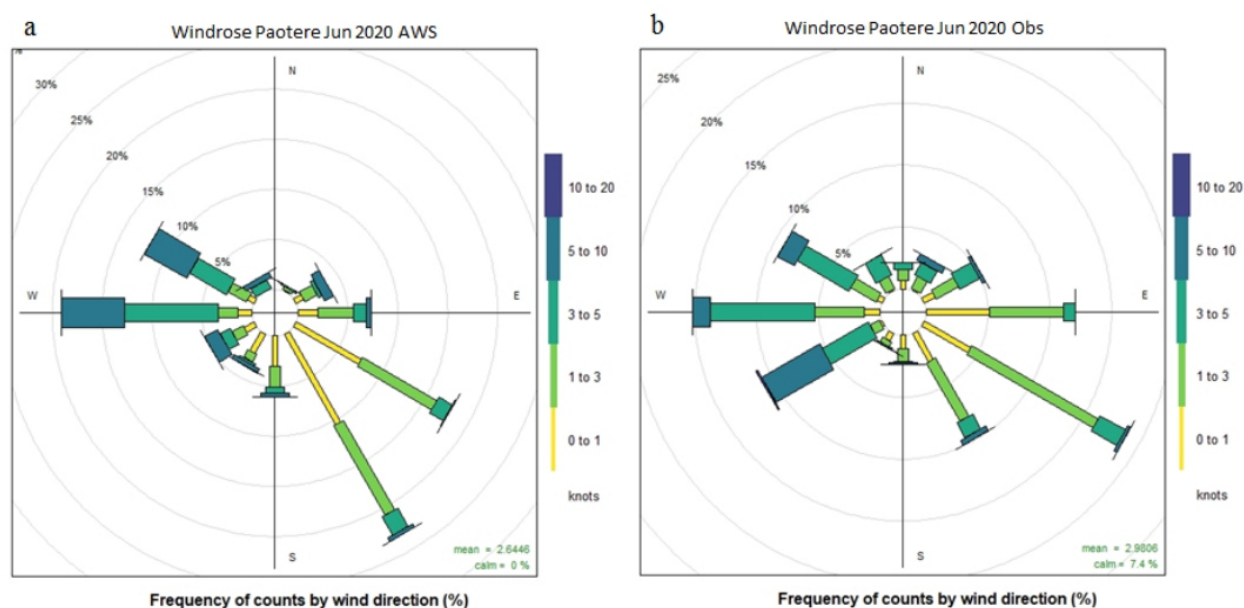


Figure 3. Windrose AWS (a) and manual (b) June 2020.

In the rainy season, the dominant wind direction comes from the west, but the east wind is the second most common in Makassar. This condition is a consequence of Makassar's location on the seafloor, so that the influence of land-sea winds is evident, both AWS and manual data. The influence of the land sea breeze is always there in the rainy season months such as January, as well as in the dry season in June. In the dry season, where the east wind is dominant, it is seen in June, but the wind is both westerly. There are always east and west winds due to the location of the city of Makassar facing west on the ocean, which can be seen in the emergence of land-sea wind circulation. When viewed from the deviation of the wind speed, it seems that the magnitude of the wind speed in January has an effect on the homogeneity test.

The difference in measurement results between AWS and manual can also be seen from the boxplot graph that describes the quantile distribution. Data with high disparity means the quantile value will be very different from data with low distribution. The distribution of quantile values for each AWS and manual parameter can be seen in Figures 6 to 13.

The pressure values in January between AWS and manual are almost the same as in Figure 4, while there are slightly different in June. Manually measuring pressure results in slightly lower values than using AWS. The range of automatic measurement is also slightly higher than that of manual measurement as shown in Figure 5.

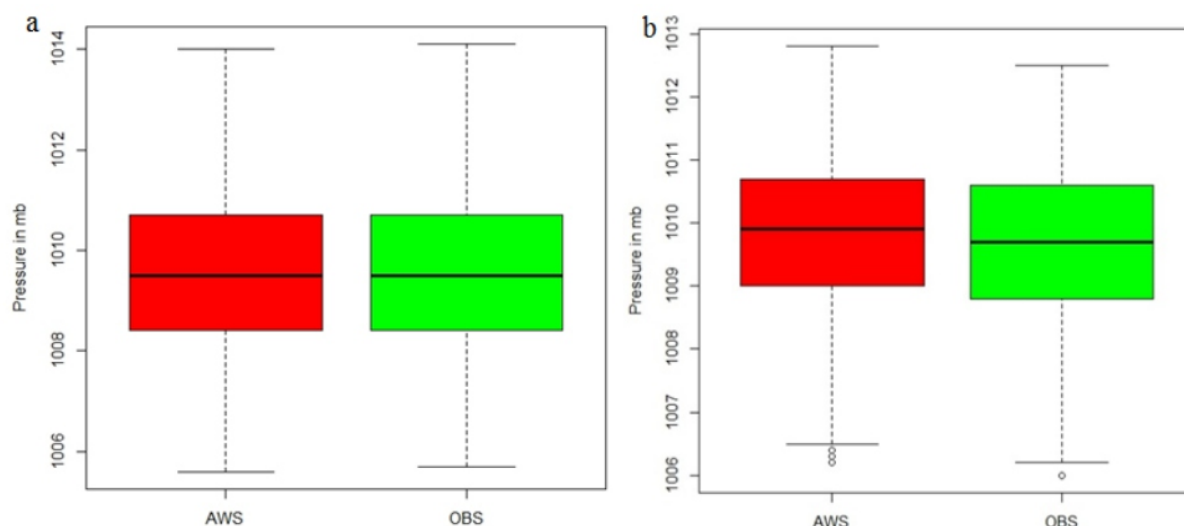


Figure 4. Comparison boxplot of pressure January (a) and June (b) 2020.

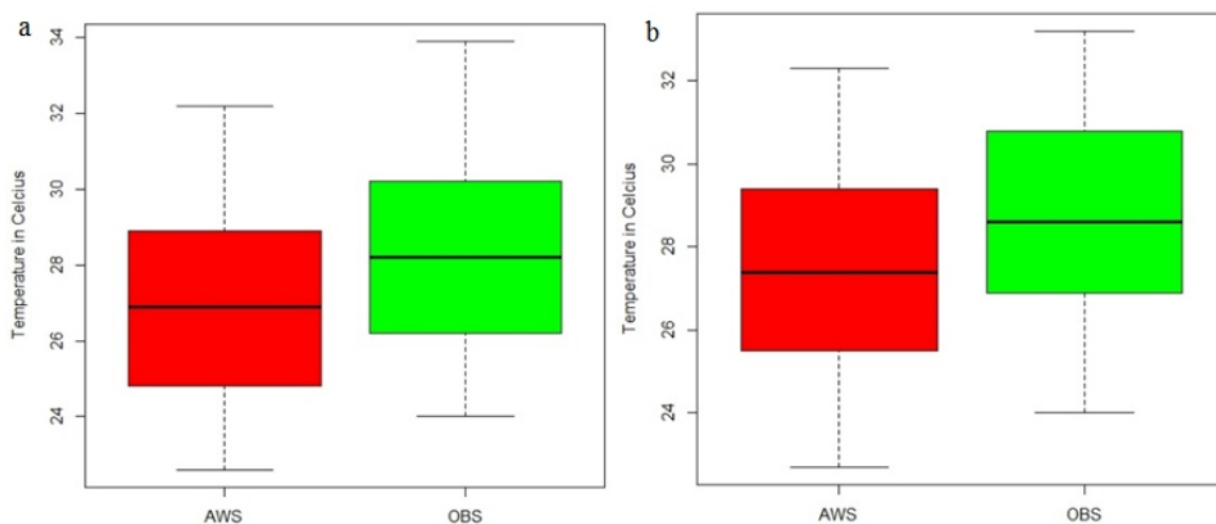


Figure 5. Comparison boxplot of temperature January (a) and June (b) 2020.

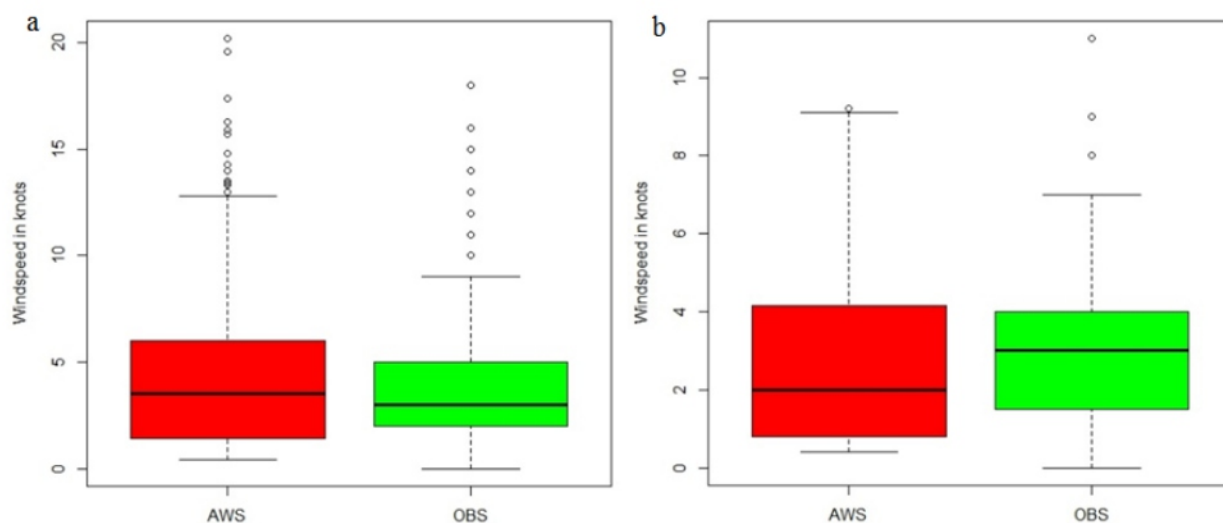


Figure 6. Comparison boxplot of wind speed January (a) and June (b) 2020.

Temperatures in January and June on measurements using AWS and manual have almost the same pattern as in Figure 6. The results of manual measurements are slightly higher than those of automatic measurements. The median and first and third quantile values in manual observations tend to be higher than AWS, both in January and June.

A different pattern was found in wind speed measurements, where in January, AWS data showed a very high disparity compared to manual observations. Meanwhile, in June this measurement disparity is smaller compared to January which has a lot of rain as shown in Figure 6. The rainfall homogeneity test resulted in a non-homogeneous conclusion in January and June. The difference will be clearer by comparing the two measurements using a plot series of rainfall data as shown in Figures 7 and 8. Generally, the manual measurement results were much higher in the month where rainfall fell a lot, namely January which was seen in Figure 7. When the rainfall value is 30 mm/hour, AWS records a smaller value than the manual. Even in the event of rain with an intensity of more than 60mm/hour, the AWS value is very small compared to the manual rainfall rate.

Rain detection on AWS and manual looks better in the dry season in June. Only when it rains below 1 mm/hour, where manual equipment does not record rain, AWS is more sensitive to recording rainfall. However, it seems that the sensitivity of AWS equipment in the dry season is reduced when the rainfall is more than 4 mm/hour. When the rainfall has high intensity, AWS slow records the rainwater that enters the device. This may be because the tipping bucket movement did not record rainfall. However, if you look at the amount of rain the next day, it seems that the lack of rainfall on AWS will be recorded the next day as shown in Figure 8.

The conditions are different compared to June where the rainfall is not too much. This month the boxplot chart shows a higher variance in the AWS measurements than the manual, although in fact the rainfall values may be almost the same. In June, the intensity of rain fell is low, this makes it somewhat sensitive to variance so that the homogeneity test shows that it is not homogeneous. The boxplot results on humidity are almost the same as the temperature boxplot, where the manual data pattern is lower than AWS as shown in Figure 9.

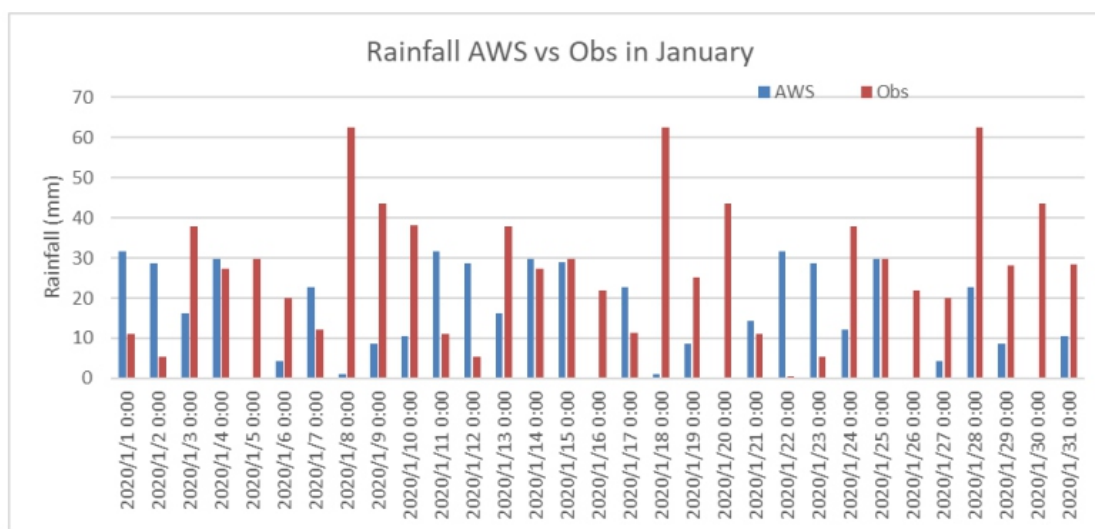


Figure 7. Comparison histogram of rainfall January 2020.

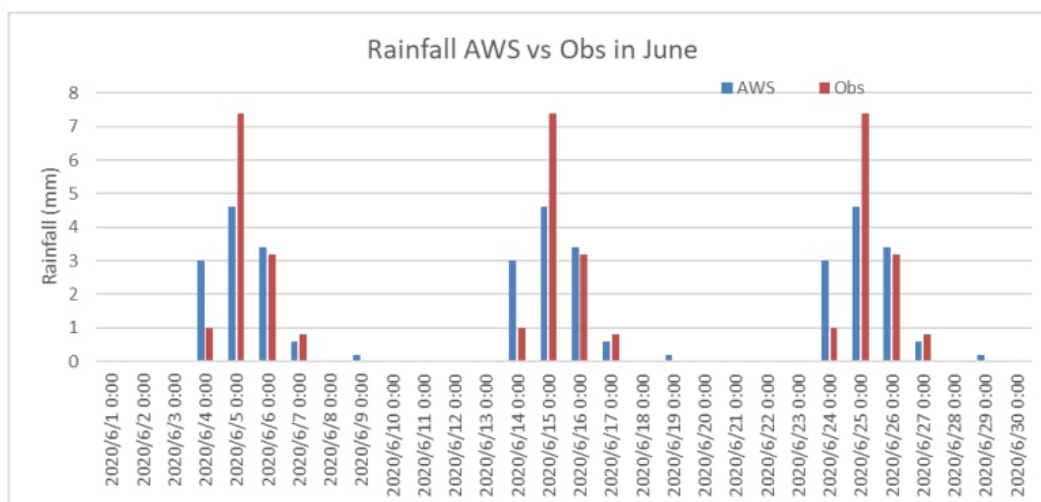


Figure 8. Comparison histogram of rainfall June 2020.

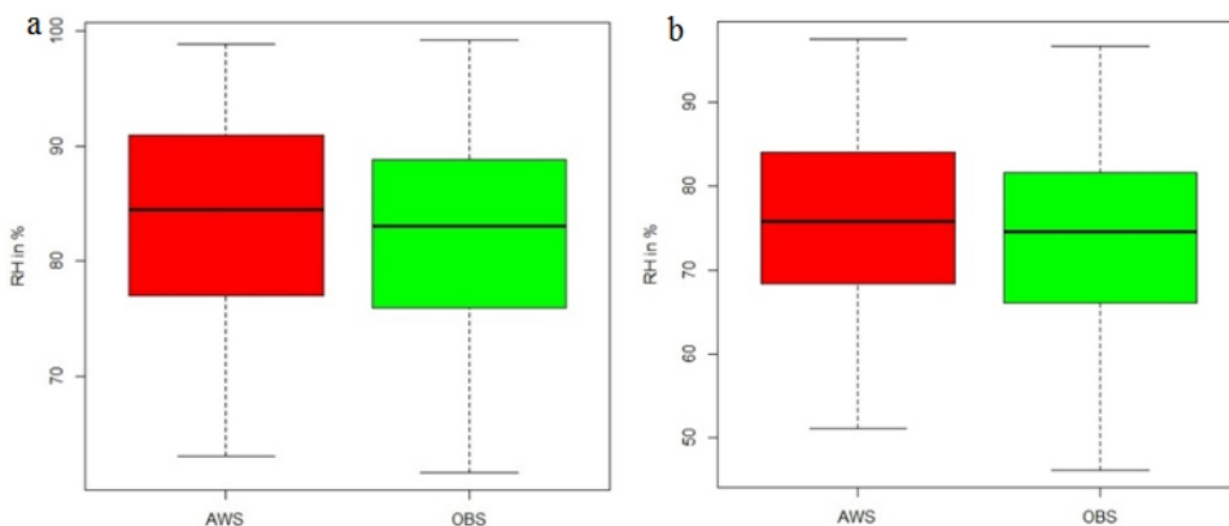


Figure 9. Comparison boxplot of humidity January (a) and June (b) 2020.

4. Discussion

The results of manual measurements and AWS produce data that is partially homogeneous, but sometimes also not homogeneous. In the rainy season, the difference between the two types of measurements is greater than in the dry season. Based on the boxplot graph, it shows changes in variability due to the magnitude of the measured parameter values, where humidity and rain are very sensitive to the disparity of measured values.

In January the pressure on AWS was about the same as the manual. In addition, based on the homogeneity test and boxplot graphs, it is shown that the two measurements are very similar. However, this condition changes during the dry season, where the pressure on AWS is higher than the manual results. Based on the temperature boxplot graph which shows the higher AWS temperature disparity compared to manual, it is suspected that it will have an effect on the air density at the location where the equipment is installed. Due to the air density affecting the pressure, automatically in June this air pressure also experienced a disparity in value between AWS and manual. Rapid changes in air are caused by the lack of water vapor content that can store latent heat which results in rapid changes in air

pressure. However, this change is not too much value at temperature and pressure. The quantiles of temperature and pressure during the dry season are around the average.

In contrast to humidity, which during the rainy season tends to be very high in value or wetter when it rains, and then decreases when it is sunny, the disparity during the rainy season is higher than during the dry season. As a result, the homogeneity test during the rainy season, AWS and manual homogeneity tests concluded that it was not homogeneous. The location and elevation of the AWS sensors near the sea may have an effect on the rapid changes in air properties around the seaside compared to areas that are further away such as in the tool park, especially between the tool park and the AWS sensor there is a separator that is sufficient to block the wind. Both AWS and manual observations show that the influence of land-sea winds in Makassar is very strong. During the rainy season, where the dominant wind direction should only be from the west or around the west, but the easterly wind appears to be the second most common in Makassar. Both AWS and manual observations show the same result. This is reinforced during the dry season, where the east wind or around the east should be very dominant, but the results of the analysis show that in June the dominant wind is both westerly winds. There are always east and west winds due to the location of the city of Makassar facing west on the ocean, which can be seen in the emergence of land-sea wind circulation. When viewed from the deviation of the wind speed, it seems that the magnitude of the wind speed in January has an effect on the homogeneity test.

Precipitation is the most consistently different weather parameter between manual measurement and automatic observation or AWS. Both in January and June obtained the homogeneity test resulted in a non-homogeneous conclusion. In both rainy and low-rainy months, manual measurement is higher than automatic measurement. The disparity between the two types of measurement results in an inhomogeneous between AWS and manual. Based on the properties of these two types of measurements, it is possible to distort the results of observations. The first is time resolution, where AWS records every 10 minutes while manual observations every hour. In manual measurements, rain is even recorded every three hours so that the temporal resolution is very different. The AWS rain gauge type is tipping bucket, while manual observation is capped using gauge degrees. The second, according to the technician, there is a possibility that the electric current will weaken so that the rainfall record will be disrupted when the intensity of rainfall starts to increase. However, the comparison in this research uses data every 3 hours so that the AWS and manual rainfall values should not be much different. But given the inhomogeneity of the two and the obvious differences there are likely AWS tools to look out for.

5. Conclusions

Based on the comparative analysis of AWS and manual measurements, the homogeneity of these two types of measurements can change at any time with the following details:

- 1) During the rainy season, only pressure and temperature are identical and homogeneous. Meanwhile, in the dry season, apart from these two parameters, humidity and wind speed are also homogeneous and rainfall is an unstable parameter in January and June. The homogeneity test is very sensitive to very different values, where humidity and rainfall are very sensitive to the disparity of measured values.
- 2) Both AWS and manual observations show that the influence of land-sea winds in Makassar is very strong. During the rainy season, where the dominant wind direction should only be from the west or around the west, but the easterly wind appears to be the second most common in Makassar.
- 3) Both AWS and manual observations show the same result. This is reinforced during the dry season, where the east wind or around the east should be very dominant, but the results of the analysis show that in June the dominant wind is both westerly winds.
- 4) There are always east and west winds due to the location of Makassar city which faces west on the

ocean, it can be seen in the emergence of land-sea wind circulation. The homogeneity test is very sensitive to very different values, where humidity and rainfall are very sensitive to the disparity of measured values.

AWS and manual observations show that the influence of land-sea winds in Makassar is very strong. During the rainy season, where the dominant wind direction should only be from the west or around the west, however, the easterly wind appears to be the second most common in Makassar. This is reinforced during the dry season, where the east wind or around the east should be very dominant, but the results of the analysis show that in June the dominant wind is both westerly winds. There are always east and west winds due to the location of Makassar city which faces west on the ocean, it can be seen in the emergence of land-sea wind circulation.

Conflict of interest

All authors declare no conflicts of interest in this paper.

References

1. Sunusi N, Giarno (2022) *Comparison of some schemes for determining the optimal number of rain gauges in a specific area: A case study in an urban area of South Sulawesi, Indonesia*. *AIMS Environ Sci* 9: 260–276. <http://doi.org/10.3934/environsci.2022018>
2. Giarno, Muflihah, Mujahidin (2020) *Determination of optimal rain gauge on the coastal region use coefficient variation: Case study in Makassar*. *J Civ Eng Forum* 7: 121–132. <https://doi.org/10.22146/jcef.58378>
3. WMO (2017) *Challenges in the Transition from Conventional to Automatic Meteorological Observing Networks for Long-term Climate Records*. Available from: https://library.wmo.int/doc_num.php?explnum_id=4217.
4. WMO (1994) *Guide to Hydrological Practices: Data Acquisition and Processing, Analysis, Forecasting and Other Applications*. Available from: https://portal.camins.upc.edu/materials_guia/250144/2013/WMOENG.pdf.
5. WMO (2008) *Guide to Meteorological Instruments and Methods of Observation*. Available from: <https://www.posmet.ufv.br/wp-content/uploads/2016/09/MET-474-WMO-Guide.pdf>.
6. Milewska E, Hogg WD (2002) *Continuity of climatological observations with automation temperature and precipitation amounts from AWOS (Automated Weather Observing System)*. *Atmos Ocean* 40: 333–359. <https://doi.org/10.3137/ao.400304>
7. Zahumenský I (2004) *Guidelines on Quality Control Procedures for Data from Automatic Weather Stations*. Available from: https://www.researchgate.net/publication/228826920_Guidelines_on_Quality_Control_Procedures_for_Data_from_Automatic_Weather_Stations.
8. Wang Y, Liu XN, Ju XH (2006) *Differences between automatic and manual meteorological observation*. *TECO-2006–WMO Technical Conference on Meteorological and Environmental Instruments and Methods of Observation*.
9. Wang Y, Liu XN, Ren ZH (2006) *Initial analysis of AWS-observed temperature*. *TECO-2006–WMO Technical Conference on Meteorological and Environmental Instruments and Methods of Observation*.
10. Guttman RNB, Baker CB (1996) *Exploratory analysis of the difference between temperature observations recorded by ASOS and conventional methods*. *B Am Meteorol Soc* 77: 2865–2873. [https://doi.org/10.1175/1520-0477\(1996\)077%3c2865:EAOTDB%3e2.0.CO;2](https://doi.org/10.1175/1520-0477(1996)077%3c2865:EAOTDB%3e2.0.CO;2)
11. Brandsma T (2011) *In: Parallel air temperature measurements at the KNMI-trrain in De Bilt (the Netherlands) May 2003–April 2005, interim report*. Netherlands: KNMI.

12. Sunusi N, Herdiani ET, Nirwan I (2017) Modeling of extreme rainfall recurrence time by using point process models. *J Environ Sci Technol* 10: 320–324. <https://doi.org/10.3923/jest.2017.320.324>
13. Aprilina K, Nuraini TA, Sopaheluwakan A (2017) Preliminary statistical assesment of temperature data obtained from parallel automatic and manual observation. *JMG* 18: 13–20.
14. Giarno, Hadi MP, Suprayogi S, et al. (2018) Distribution of accuracy of TRMM daily rainfall in Makassar Strait. *For Geo* 32: 38–52. <http://doi.org/10.23917/forgeo.v32i1.5774>
15. Wang ZL, Zhong RD, Lai CG, et al. (2017) Evaluation of the GPM IMERG satellite-based precipitation products and the hydrological utility. *Atmos Res* 196: 151–163. <https://doi.org/10.1016/j.atmosres.2017.06.020>
16. Tapiador FJ, Navarro A, Ortega EG, et al. (2020) The contribution of rain gauges in the calibration of the IMERG product: Results from the first validation over Spain. *J Hydrometeorol* 21: 161–182. <https://doi.org/10.1175/jhm-d-19-0116.1>
17. Tokay A, Petersen WA, Gatlin P, et al. (2013) Comparison of raindrop size distribution measurements by collocated disdrometers. *J Atmos Ocean Tech* 30: 1672–1690. <https://doi.org/10.1175/JTECH-D-12-00163.1>
18. Piticar A, Ristoiu D (2012) Analysis of air temperature evolution in northeastern Romania and evidence of warming trend. *Carpathian J Earth Environ Sci* 7: 97–106.
19. Gentilucci M, Moustafa AA, Gawad FK, et al. (2021) Advances in Egyptian mediterranean coast climate change monitoring. *Water* 13: 1870. <https://doi.org/10.3390/w13131870>
20. Wijngaard JB, Klein Tank AMG, Können GP (2003) Homogeneity of 20th century European daily temperature and precipitation series. *Int J Climatol* 23: 679–692. <https://doi.org/10.1002/joc.906>
21. Farrell PJ, Stewart RK (2006) Comprehensive study of tests for normality and symmetry: Extending the spiegelhalter test. *J Stat Comput Sim* 76: 803–816. <https://doi.org/10.1080/10629360500109023>
22. Majid AS, Dharmawan GSB, Heryanto DT, et al. (2017) Automation of surface observing network in BMKG. *The WMO International Conference on Automatic Weather Stations (ICAWS-2017)*.
23. Ranalkar M, Gupta M, Mishra R, et al. (2014) Network of automatic weather stations: Time division multiple access type. *Mausam* 65: 393–406. <https://doi.org/10.54302/mausam.v65i3.1048>
24. Chan PW, Shun CM (2007) Comparison of manual observations and instrumental readings of visibility at the Hong Kong International Airport. *Hong Kong Meteorol Soc Bull* 17: 94–98.
25. Petersen JF, Sack D, Gabler RE (2011) In: *Fundamentals of physical geography*, Boston: Cengage Learning.
26. Karaseva MO, Prakash S, Gairola RM (2012) Validation of high-resolution TRMM-3B43 precipitation product using rain gauge measurements over Kyrgyzstan. *Theor Appl Climatol* 108: 147–157. <https://doi.org/10.1007/s00704-011-0509-6>
27. Prasetya R, As-syakur AR, Osawa T (2013) Validation of TRMM precipitation radar satellite data over Indonesian region. *Theor Appl Climatol* 112: 575–587. <https://doi.org/10.1007/s00704-012-0756-1>
28. Scheel MLM, Rohrer M, Huggel C, et al. (2011) Evaluation of TRMM multi-satellite precipitation analysis (TMPA) performance in the central Andes region and its dependency on spatial and temporal resolution. *Hydrol Earth Syst Sci* 15: 2649–2663. <https://doi.org/10.5194/hess-15-2649-2011>
29. Guo H, Chen S, Bao AM, et al. (2016) Comprehensive evaluation of high-resolution satellite based precipitation products over China. *Atmosphere* 7: 6. <https://doi.org/10.3390/atmos7010006>
30. Saber M, Yilmaz K (2016) Bias correction of satellite-based rainfall estimates for modeling flash floods in semi-arid regions: Application to Karpuz River, Turkey. *Nat Hazards Earth Syst Sci Discuss*. In press. <https://doi.org/10.5194/nhess-2016-339>
31. Tan ML, Ibrahim AL, Duan Z, et al. (2015) Evaluation of six high-resolution satellite and ground

based precipitation products over Malaysia. Remote Sens 7: 1504–1528.<https://doi.org/10.3390/rs70201504>

32. McCarroll D (2016) *In: Simple statistical tests for geography*, Boca Raton: CRC Press.

33. EGU (2017) *European Geosciences Union General Assembly 2017. Available from: <https://meetingorganizer.copernicus.org/EGU2017/orals/22780>.*

A Study of Infaunal Abundance, Diversity and Distribution in Chettuva Mangrove, Kerala, India

Rukhsana Kokkadan^{1,*}, Resha Neznin¹, Praseeja Cheruparambath², Jerisa Cabilao¹ and Salma Albouchi

¹ Nautica Environmental Associates LLC, Abu Dhabi, United Arab Emirates

² Department of Zoology, SN College, Alathur, Kerala, India

ABSTRACT

This study investigates an account on the diversity and abundance of benthic infauna of Chettuva mangrove in Kerala. Marine benthic infaunal species are an important factor in marineeco systems and play a chiefecological function in the mangrove ecosystem. This research articlegives an overview of infaunal diversity associated with eight sites of Chettuva mangrove. Thepresent study revealed that infaunal species are significantly moderate within this mangroveecosystem.

Keywords: *Polychaetes; infauna; mangrove; population density; statistical analysis*

1. Introduction

Mangroves are a precise coastal ecosystem contributing as a wealthy store of resident biodiversity. The diversity of the benthic infauna is largely underestimated and must undergo regular revision in order to detect and monitor changes of benthic communities within the area.

The benthic communities constitute a dominant component that supports habitat productivity to a greater extent. Due to this, the species composition may negatively affect the resident community and consequently impact trophic relationships within these communities as a result of any activity exerted, causing a change for sediment features [1,2]. Zainal et al. and Ali et al. pointed out that the macrobenthic faunal diversity around the Huwar islands [3,4] and Bahrain are very important in ecosystem balancing. Other regions, such as Europe [5,6], North America [7,8] and South Africa, have produced monographs for faunal identification [9]. However, most of the benthic faunal communities have not yet been thoroughly explored in India.

Kerala is gifted with a long coastal line and extensive estuaries. Estuarine water contains a rich supply of nutrients. No comprehensive study has been done so far on benthic infaunal biodiversity and abundance in this Chettuva mangrove area.

2. Material and methods

2.1. Collection of water and sediment samples

The present study was designed to characterize the benthic infauna community of eight different sites in Chettuva mangrove, Kerala, as seen in Figure 1. Biological samples from each station, three replicate samples, were collected using benthic grab sampler. The procedure adopted for sampling was following the method of Mackie [10]. After collecting the samples, they were emptied into a plastic tray. The larger organisms were handpicked (extracted) immediately from the sediments and then sieved through 0.5 mm mesh screen. The organisms retained by the sieve were placed in a labelled container and fixed in 5%–7% formalin. Subsequently, the organisms were stained with Rose Bengal solution (0.1 g in 100 ml of distilled water) for greater visibility during sorting. All the species were

sorted, enumerated and identified to the advanced possible level with the consultation of available literature. The works of Fauvel and Day and <http://www.marinespecies.org/polychaeta/> were referred for identification [11].



Figure 1. A Chettuva Mangrove map showing eight different sites of collection.

2.2. Statistical analyses

Statistical software was used to analyze the data obtained from different sites [12]. This was done using various statistical methods, such as univariate, multivariate and graphical/distributional methods. Biodiversity indices were calculated for the infaunal community, which included diversity index (H') using the method of Shannon-Wiener's [13] formula, species richness (d) using the Margalef [14] formula and species evenness (J') using the Pielou [15] formula. Similarities (or dissimilarities) between sites were obtained showing the interrelationships of all through an MDS plot (non-metric Multi-Dimensional Scaling) [16,17]. Cluster analysis was also done to calculate the similarities. All the various statistical methodologies and calculations were obtained through the software PRIMER V7 (Plymouth Routines in Multivariate Ecological Research) developed by Plymouth Marine Laboratory.

3. Results

3.1. Species Composition in Chettuva Mangrove

A total of 339 organisms were identified from eight samples, spanning 40 taxa from four phyla (Tables 1 & 2), representing an average of 42 specimens per sample. The species composition by phylum within the Chettuva Mangrove area was predominated by annelids with 72.27% (Figure 2). Arthropods formed the second most important group, represented by 15.93%. Mollusca constituted 9.73%, and the fourth important group was the Echinodermata, which comprised of 2.06%. Annelids composed the majority of the infaunal species composition (Table 1).

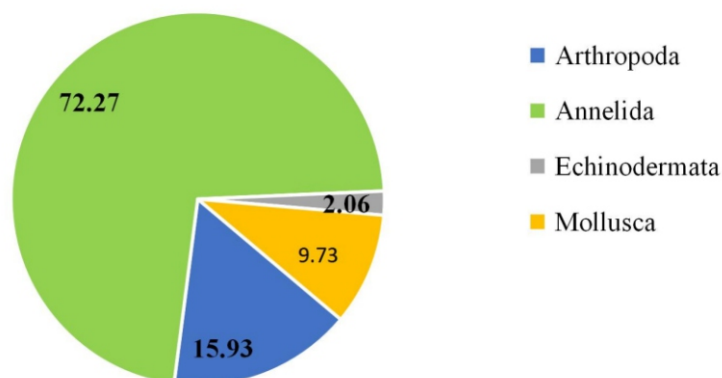


Figure 2. Infauna species composition by phylum level in the Chettuva Mangrove area.

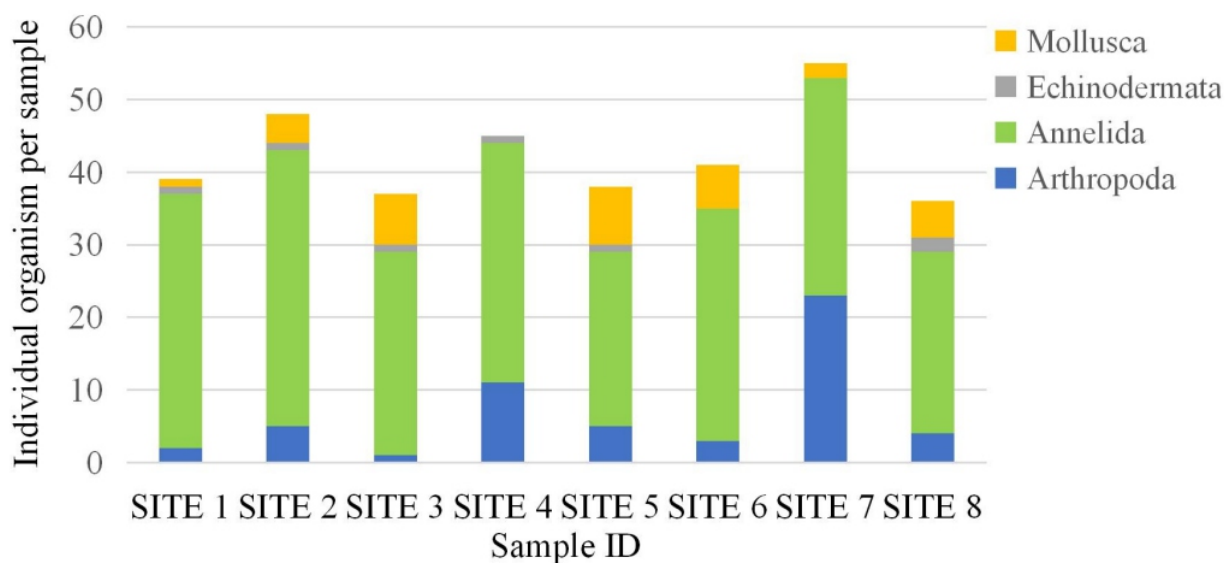


Figure 3: Total number of individuals per site.

Among all the eight stations, Site 7 is the most abundant and diverse, with 55 individuals across 19 taxa. Capitellidae was the most numerous family, indicating a clear dominance. Samples with common abundant taxa are presented in Figure 3. Within the polychaetes, Capitellidae, Opheliidae, Spionidae and Terebellidae were found to be the most recurring species in the samples collected within this mangrove ecosystem. With respect to arthropods, Anoplodactylus sp. and Apseudidae were the most abundant species.

Table 1. Taxonomic breakdown of infauna in the Chettuva Mangrove area.

Phylum	Number of Taxa	Relative abundance (%)
Annelida	22	72.27
Arthropoda	13	15.93
Mollusca	4	9.73
Echinodermata	1	2.06
Total	40	100



Figure 4. Branchiostoma lanceolatum, Terebellidae, Capitellidae, Anoplodactylus sp., Sabellidae, and Lumbrineridae

3.2. Dominance

Figure 5 represents the k-dominance curves for each station at each area. These plots illustrate the cumulative abundance of infauna plotted against the species rank. The curves are formulated from both a richness measure (species rank) and an evenness measure (% cumulative dominance).

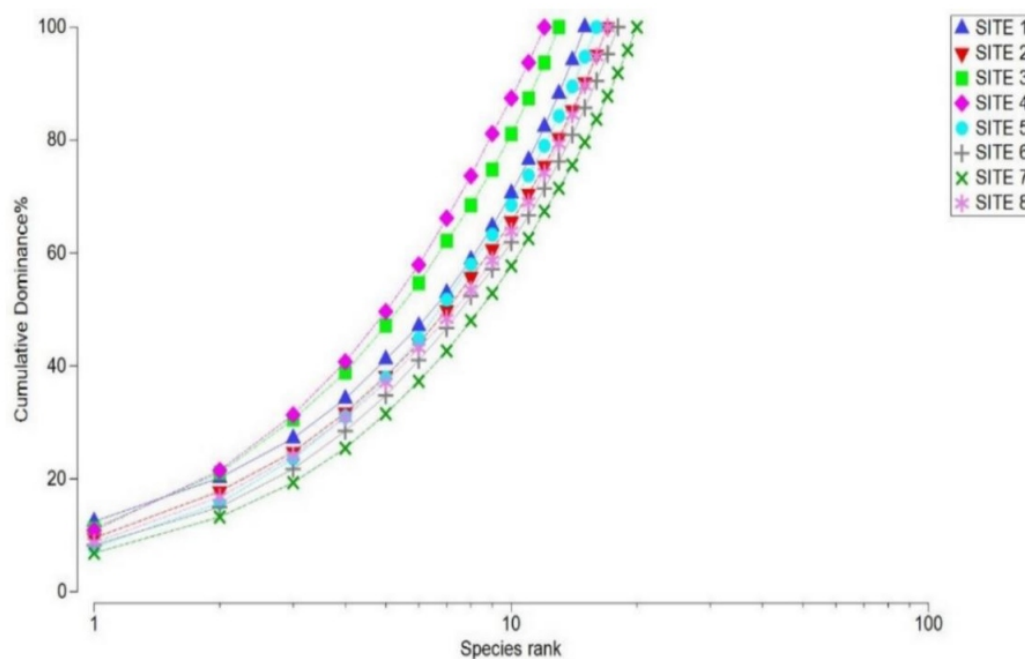


Figure 5. Dominance plots of benthic Infaunal taxa in the Chettuva Mangrove area.

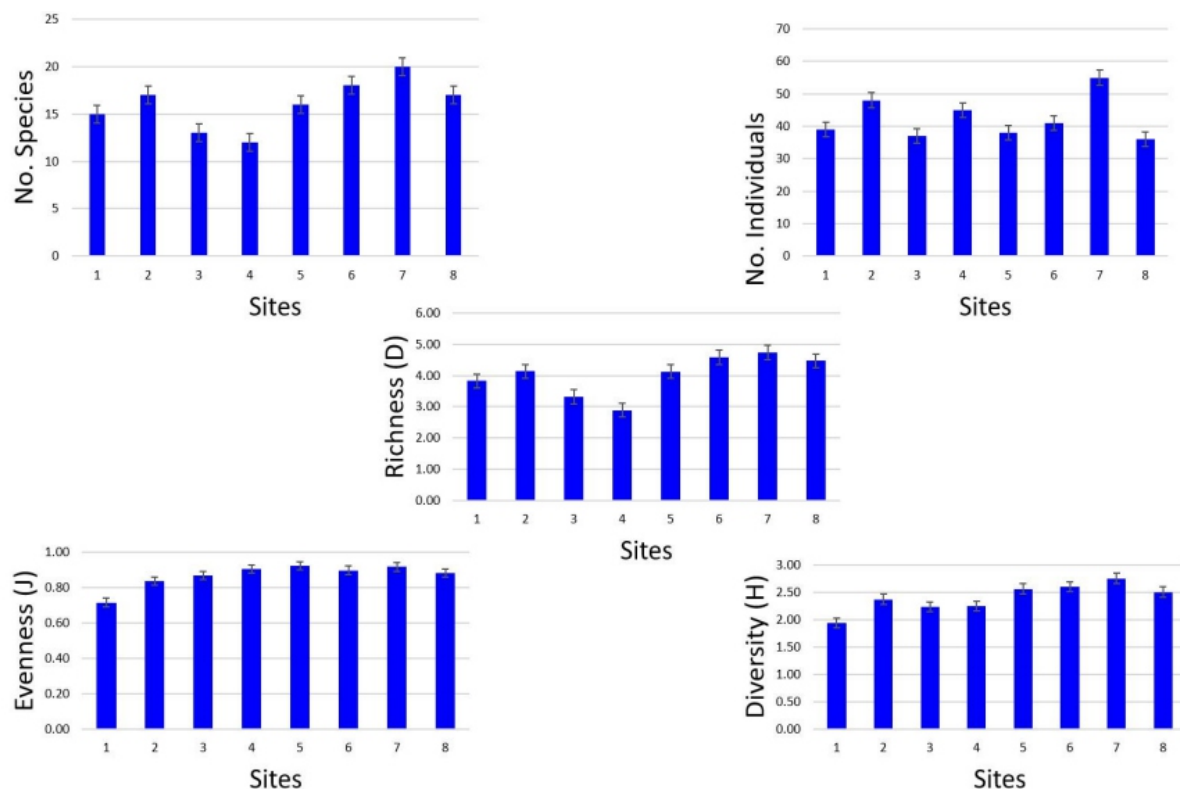


Figure 6. Biodiversity indices of infaunal benthic community in the Chettuva Mangrove area.

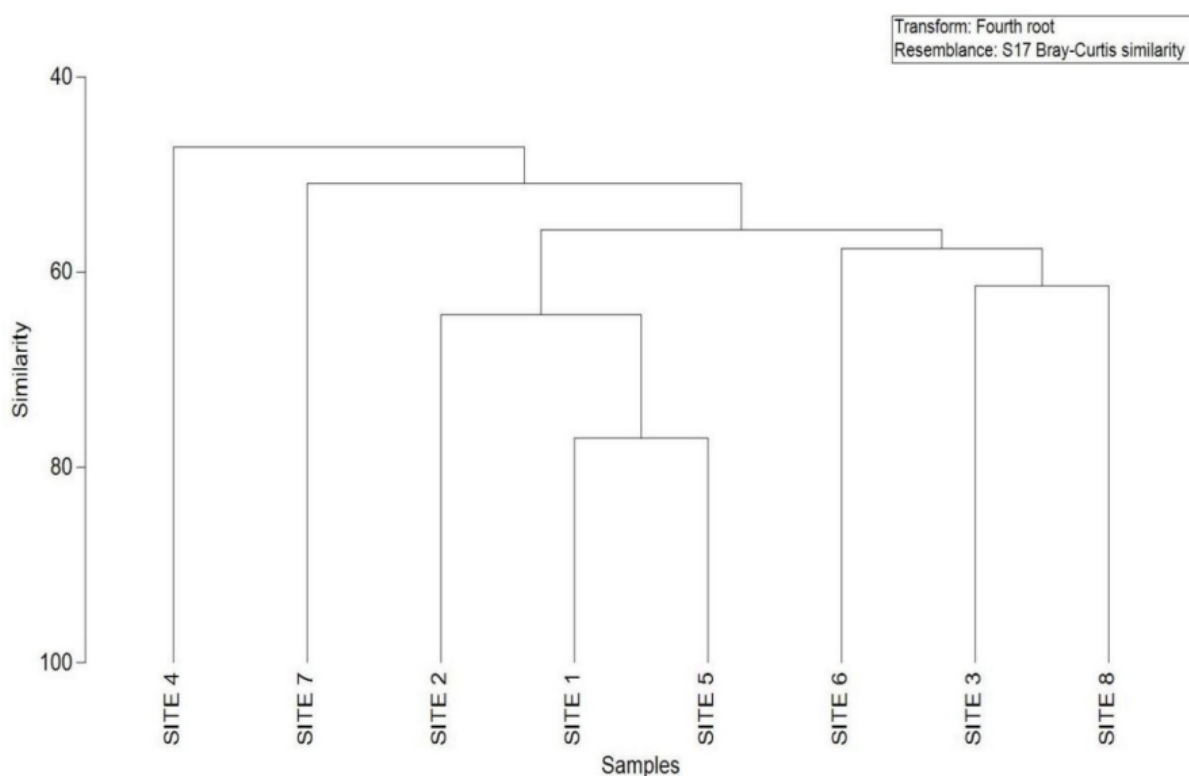


Figure 7. Dendrogram of benthic infaunal communities by site, based on

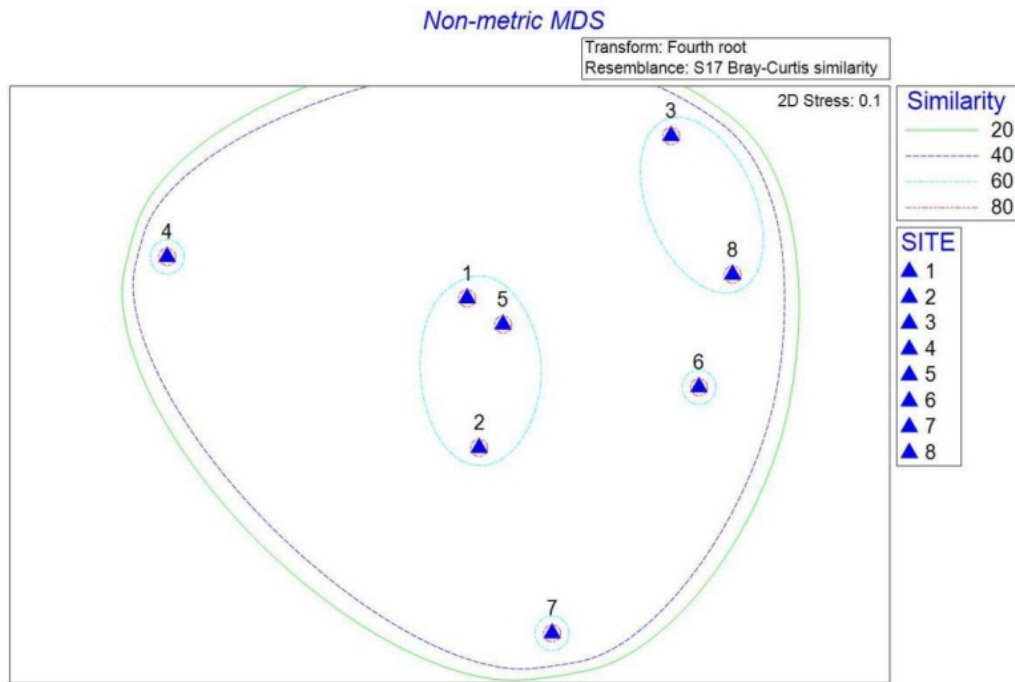


Figure 8: MDS Plot of benthic infaunal communities by site, based on Bray-Curtis similarity.

The results of the dendrogram show that species from these eight sites were grouped to two major categories (Figure 7). Among these sites, site 4, site 6, and site 7 form a separate group while all other sites are branched to from a major group.

Table 2. Infaunal taxa and its distribution in the Chettuva Mangrove area.

Taxon	SITE 1	SITE 2	SITE 3	SITE 4	SITE 5	SITE 6	SITE 7	SITE 8
<i>Golfingia</i> sp.	-	4	1	-	-	-	1	4
Sipunculidae	-	1	-	2	-	1	-	-
<i>Phascolosoma</i> sp.	-	1	1	-	1	-	-	-
Phyllodoceidae	1	-	1	-	-	1	-	-
Nephtyidae	-	-	-	-	-	1	3	-
Syllidae	1	2	-	-	3	-	5	-
Nereididae	-	-	2	-	-	4	-	1
Sigalionidae	-	2	-	3	-	-	-	-
Polynoidae	1	-	-	-	1	-	-	-
Glyceridae	2	-	-	1	3	-	-	-
Maldanidae	-	1	-	-	-	-	-	-
Lumbrineridae	2	1	-	5	1	1	3	2
Opheliidae	1	2	3	1	5	9	2	1
Spionidae	1	-	10	9	2	1	-	1
Capitellidae	20	14	5	6	5	4	8	6
Magelonidae	-	-	-	-	-	-	-	1
Orbiniidae	1	8	-	-	1	3	5	-
Terebellidae	1	1	3	2	1	4	2	8

Flabelligeridae	-	-	-	-	-	-	-	-
Cirratulidae	1	-	-	-	-	1	-	-
Amphinomidae	-	-	2	-	-	-	-	-
Sabellidae	3	1	-	4	1	2	1	1
<i>Anoplodactylus</i> sp.	2	4	1	-	5	1	6	1
Hyalidae	-	1	-	-	-	-	1	-
Melitidae	-	-	-	3	-	-	4	-
Isaeidae	-	-	-	-	-	-	-	1
Ampeliscidae	-	-	-	-	-	-	1	1
<i>Urothoe brevicornis</i>	-	-	-	-	-	-	2	-
Leptanthuridae	-	-	-	-	-	-	-	1
<i>Accalathura borradailei</i>	-	-	-	-	-	1	-	-
Cirolanidae	-	-	-	-	-	-	-	-
Bodotriidae	-	-	-	-	-	-	2	-
<i>Paranebalia</i> sp.	-	-	-	-	-	-	1	-
Apseudidae	-	-	-	8	-	1	5	-
Paratanaidae	-	-	-	-	-	-	1	-
Amphiuridae	1	1	1	1	1	-	-	2
Ancillariidae	-	1	1	-	4	2	1	3
Pteriidae	-	-	-	-	1	-	-	-
Veneridae	-	-	-	-	-	3	-	1
Tellinidae	1	3	6	-	3	1	1	1

Table 3 shows the total abundance per site, number of species and their diversity indices; Margalef species richness, Pielou species evenness and the Shannon-Weiner diversity index. Graphs of the biodiversity indices by site can be seen in Figure 6.

The three indices provide an indication of the diversity of each of the samples based on the number of species, number of individuals and the distribution of individuals between species. A more settled community will generally have a greater number of species with individuals spread more evenly between them, while a stressed or recovering community will tend to be numerically dominated by a small number of species and have fewer species overall.

Margalef species richness index (d) is heavily influenced by the overall number of species measured, though it makes a slight allowance for the number of individuals. Higher values indicate a greater number of species per individual. Margalef species richness index (d), values are ranged between 2.89 and 4.74 showing reasonably moderate to high richness. Pielou's species evenness index (J') reflects the level of spread of the individuals between the species and lies between 0 (uneven) and 1 (even). The Shannon-Weiner diversity index (H') lies between 1.94 to 2.75, indicating an average diversity. The total number of species and individuals present was influenced by salinity regimes, sediment types, organic content food availability [18]. etc. Overall, the range of species present in all samples combined suggests a moderately high level of diversity [19–22].

Multivariate analyses were conducted to investigate resemblances in the infaunal assemblages between sites across the study area (Clarke and Gorley). A Bray-Curtis (BC) similarity matrix was used to calculate the percentage similarity between all infaunal sites based on all the species present and their abundances. The samples from each site were summed so that the focus of the analysis was on similarities and differences between locations. To ensure better representation for presence/absence of taxa rather than the analysis being dominated by the most numerous species, a fourth-root

transformation was applied.

Table 3. Infaunal abundance and univariate diversity indices of all sites

Site ID	No. of Taxa (s)	No. of Individuals (n)	Margalef Species Richness (d)	Pielou Species Evenness (J')	Shannon-Weiner Diversity (log _e)(H')
SITE 1	15	39	3.82	0.72	1.94
SITE 2	17	48	4.13	0.84	2.37
SITE 3	13	37	3.32	0.87	2.23
SITE 4	12	45	2.89	0.91	2.25
SITE 5	16	38	4.12	0.92	2.56
SITE 6	18	41	4.58	0.90	2.60
SITE 7	20	55	4.74	0.92	2.75
SITE 8	17	36	4.47	0.88	2.50
Average by site	16	42	4.01	0.87	2.40

To assist with visualizing relationships between sites, the BC values have been displayed as a dendrogram (group average), in which sites where the communities are more comparable (i.e., have a higher percentage similarity value) split from one another further down the diagram.

Table 4: Similarity Percentage of site

	SITE 1	SITE 2	SITE 3	SITE 4	SITE 5	SITE 6	SITE 7	SITE 8
SITE 1	-	-	-	-	-	-	-	-
SITE 2	59.601	-	-	-	-	-	-	-
SITE 3	51.726	55.286	-	-	-	-	-	-
SITE 4	55.143	48.329	40.422	-	-	-	-	-
SITE 5	76.999	69.116	59.144	49.716	-	-	-	-
SITE 6	61.097	52.862	55.576	47.677	55.462	-	-	-
SITE 7	48.443	62.275	38.993	43.931	52.765	53.200	-	-
SITE 8	53.663	55.334	61.420	45.064	56.319	59.580	49.866	-

The BC values are also used to create Multi-Dimensional Scaling plots (MDS), where sites which have similar assemblages are plotted closer together, while those that are more dissimilar are plotted further apart. Fig. 8 shows an MDS plot for the Bray-Curtis matrix (fourth rooted data), with colored symbols indicating the transect type and a line added to show the 25% similarity level to assist with interpretation.

4. Discussion and conclusions

In this study, polychaetes were found to be the predominating phylum, playing a very important role in the recycling of organic materials within the mangroves. Their biomass creates the energy needed for the survival of this ecosystem, fueling aquatic benthic feeders. Bandekar et al. [23] stated that families like Nereidae, Nephtyidae, Onuphidae, Eunicidae, Spionidae, Maldanidae, Sabellidae, etc. are the major biomass producing annelids which form as an important food source for fishes and prawns. Similarly, bivalves provide stability to soil inhabitants and their diversity and species abundance. The infaunal species found in all the sites occupy varied benthic habitats, such as, sandy, muddy and even seagrasses, indicating an adaptive feature for survival, especially among polychaetes. However,

not many studies have been conducted within the Chettuva mangroves regarding infaunal diversity to impose an assertive conclusion on this.

Although that may be the case, similar studies in other mangrove fields like Bandekar et al. in Karwar Mangrove and Sarkar et al. [24] in Sunderban Biosphere Reserve Mangroves, have concluded that polychaetes carry certain features that help in the adaptation for survival. They are known to secrete mucus protecting themselves within peculiar habitats.

Several factors play a role causing a change in infaunal diversity and abundance, like competition with epifauna, predation by epifauna, poor quality of food and chemical defense by mangroves [25–27]. Seasons affect the diversity and density mostly due to salinity, water and sediment quality, inundation and waterlogging [28].

Acknowledgments

The authors would like to thank Mr. Veryan Pappin (Nautica Environmental Associates LLC) for the support offered to complete this research.

Conflict of interest

The authors declare no conflict of interest.

References

1. Zhi QW, Ming HC, Yi ML, et al. (2018) Different effects of reclamation methods on macrobenthos community structure in the Yangtze Estuary, China. *Marine Pollution Bulletin* 127: 429–436. <https://doi.org/10.1016/j.marpolbul.2017.12.038>
2. Lv WW, Liu ZQ, Yang Y, et al. (2016) Loss and self-restoration of macrobenthic diversity in reclamation habitats of estuarine islands in Yangtze Estuary, China. *Marine Pollution Bulletin* 103: 128–136. <https://doi.org/10.1016/j.marpolbul.2015.12.030>
3. Zainal K, Al-Sayed H, Ghanem E, et al. (2007) Baseline ecological survey of Huwar islands, The Kingdom of Bahrain. *Aquat Ecosyst Health Manag* 10: 290–300. <https://doi.org/10.1080/14634980701520882>
4. Ali TS (2014) Spatial and temporal variations of marine benthic infauna community in northern and southern areas of the Kingdom of Bahrain. *Arab Gulf J Sci Res* 32: 80–92. <https://doi.org/10.51758/AGJSR-01-2014-0010>
5. Fauvel P (1923) *Polychaetes errantes. Faune de France. Paris* 5: 1–488.
6. Fauvel P (1927) *Polychaetes sédentaires. Faune de France. Paris* 16: 1–488.
7. Hartman O (1968) *Atlas of the errantiate polychaetous annelids from California.*
8. Hartman O (1969) *Atlas of the sedentariate polychaetous annelids from California.* Allan Hancock Foundation. Uni South California, LA.
9. Day JH (1967) *A monograph on the Polychaeta of Southern Africa.* British Museum of Natural History, Publication 656: 1–878. <https://doi.org/10.5962/bhl.title.8596>
10. MACKIE AY (1994) *Adercodon pleijeli* gen. et sp. nov. (Polychaeta, Ampharetidae) from the Mediterranean Sea. *Mémoires du Muséum national d'histoire naturelle* 162: 243–250.
11. Fauvel P (1953) *The fauna of India including Pakistan. Ceylon, Burma and Malaya, Annelida Polychaeta.* Allahabad.
12. Clark KR, Gorley RN (2006) *Primer v7: User Manual/Tutorial.* Plymouth: Primer-E 182.
13. Shannon CE, Wiener W (1949) *The Mathematical Theory of Communication.* Urbana: University of Illinois Press.
14. Margalef R (1958) *Information theory in ecology.* *International Journal of General Systems*

3:36–71.

15. Pielou EC (1966) *The measurement of diversity in different types of biological collections*. *Journal of Theoretical Biology* 13: 131–144. [https://doi.org/10.1016/0022-5193\(66\)90013-0](https://doi.org/10.1016/0022-5193(66)90013-0)
16. Shepard RN (1962) *The analysis of proximities: Multidimensional scaling with an unknown distance function*. *Psychometrika* 27: 125–140. <https://doi.org/10.1007/BF02289630>
17. Kruskal JB (1964) *Multidimensional scaling by optimising goodness of fit to a nonmetric hypothesis*. *Psychometrika* 29: 1–27. <https://doi.org/10.1007/BF02289565>
18. Paul VRS, Blackburn HT, Pat H, et al. (1997) *The importance of marine sediment biodiversity in ecosystems processes*. *AMBIO* 26: 578–583.
19. Simpson EH (1949) *Measurement of diversity*. *Nature* 163: 688–688. <https://doi.org/10.1038/163688a0>
20. Cootam G, Curtis JT (1956) *The use of distance measures in phytosociology sampling*. *Ecology* 37: 451–460. <https://doi.org/10.2307/1930167>
21. Gauch Jr HG (1983) *Multivariate analysis in community structure*. Cambridge University Press, Cambridge.
22. Ter Braak CJF, Prentice IC (1988) *A theory of gradient analysis*. *Advances in Ecological Research* 18: 271–313. [https://doi.org/10.1016/S0065-2504\(08\)60183-X](https://doi.org/10.1016/S0065-2504(08)60183-X)
23. Bandekar PD, Naik UG, Haragi SB (2017) *Diversity status of benthic macro polychaete species in estuarine region of Karwar, West Coast of India*. *International Journal of Fisheries and Aquatic Studies* 5: 216–219.
24. Sarkar SK, Bhattacharya A, Giri S, et al. (2005) *Spatiotemporal variation in benthic polychaetes (Annelida) and relationships with environmental variables in a tropical estuary*. *Wetlands Ecology and Management* 13: 55–67. <https://doi.org/10.1007/s11273-003-5067-y>
25. Lv WW, Huang YH, Liu ZQ, et al. (2016) *Application of macrobenthic diversity to estimate ecological health of artificial oyster reef in Yangtze Estuary, China*. *Marine Pollution Bulletin* 103: 137–143. <https://doi.org/10.1016/j.marpolbul.2015.12.029>
26. Liu ZQ, Fan B, Huang YH, et al. (2019) *Assessing the ecological health of the Chongming Dongtan Nature Reserve, China, using different benthic biotic indices*. *Marine Pollution Bulletin* 146: 76–84. <https://doi.org/10.1016/j.marpolbul.2019.06.006>
27. Dittmann S (2001) *Abundance and distribution of small infauna in mangroves of Missionary Bay, North Queensland, Australia*. *Revista de Biologia Tropical* 49: 535–544.
28. Jaritkhuan S, Damrongrojwattana P, Chewprecha B, et al. (2017) *Diversity of Polychaetes in Mangrove Forest, Prasae Estuary, Rayong Province, Thailand*. *Chiang Mai Journal of Science*, 44: 816–823.

Radioactive waste management and disposal – introduction to the special issue

María Sancho*

Instituto Universitario de Seguridad Industrial, Radiofísica y Medioambiental (ISIRYM),
Universitat Politècnica de València, Camino Vera s/n, 46022, Spain

In this special issue of AIMS Environmental Science, present trends of radioactive waste management are reviewed. In spite of nuclear energy production, radionuclides have many other important applications in medicine and industrial fields. The sustainability of all radionuclides applications depends on the proper management of radioactive wastes. The characteristics of these wastes can be very different depending on the previous application. Thus, we can find solid or liquid wastes with ranges of radioactivity from low/medium ($< 3.7 \times 10^8$ Bq) to high ($10^4 - 10^6$ TBq/m³). Nowadays, management of low/medium activity wastes is well established and mainly consists of the following basic stages:

- a) Prevention and minimization. Reduction of waste volume and activity are basic principles for environmental impact and cost decrease. In this line, short half-life radionuclides must replace long half-life ones [1], and wastes must be segregated according to solid/liquid state, radionuclide content, level of activity and half-life of radionuclides [2].
- b) Storage for decay. When it is possible, storage of radioactive wastes is used to reduce the level of activity before discharge or transport to a disposal facility.
- c) Discharge after decay. Some radioactive liquid wastes (as the ones produced in some medical applications) can be discharge to sewer after storage for decay [3], if other release criteria such as radiological, chemical and biological ones are met.
- d) Concentrate and contain. When option of delay and decay is not practical due to the level of activity and/or the length of half-lives, radioactive waste must be concentrated by a conditioning process to reduce volume and then confine the radionuclides to prevent their dispersion in the environment [4]. After this, concentrated wastes are collected in suitable containers and buried in authorized sites.

This Special Issue aims to contribute with papers on research and innovation in the field of radioactive waste treatment, both medium-low and high activity, covering topics as diverse as those related to the most advanced management procedures, which involve the systematization and implementation of integral management systems [2,5]; as well as the implementation of methods for predicting and monitoring the radiological incidence [6,7] of waste and/or its environmental impact [8,9], using dose calculation and associated risk assessment software [10,11]; or the application of specific treatments for the declassification of waste such as volume reduction prior to its disposal [12–14], among which the application of nanomaterials stands out [15].

On the other hand, an important field of research is the structures and materials that allow the long-term storage of high activity radioactive materials, both in the nuclear facilities themselves and in the final storage sites. In this sense, there is room for studies on the degradation of the containers used for storage [16]; as well as research on the application of new materials, among which those that include nanoparticles should be noted [17].

Among the sectors of origin of the waste to be managed, the scope of the special issue covers waste from the nuclear industry (spent fuel storage and reprocessing), as well as waste from industry or medical applications. On the other hand, the radiological incidence and the management of NORM Naturally Occurring Radioactive Materials (NORMs) are also considered, in spite of not being strictly waste,

since they can have a significant radiological impact. As it is the case of TENORM materials (Technologically Enhanced NORMs), which are those radioactive materials of natural origin whose exposure potential has increased compared to the situation unaltered by human technological activity. Among the TENORMs, the case of phosphate sludges coming from the phosphoric acid production industry is especially relevant since it is a very important environmental problem [18,19] for which a definitive solution has not yet been found.

Finally, among the most current trends in the field of radioactive waste, it is worth highlighting the application of biological treatments [20] such as the sequestration of radionuclides through the use of bacteria that have the capacity to adsorb them specifically; and bioremediation, through the which radioactive compounds are transformed into non-radioactive ones by the metabolic action of microorganisms. In this sense, promising results are being achieved in the sequestration of uranium [21], Sr-90 and Ra-226 [22], as well as Tc-99 [23].

Through all these relevant topics, it is hoped that this special issue contributes to make visible and promote adequate management of all radioactive waste, which allows its application in conditions of sustainability.

Conflict of interest

Author declares no conflicts of interest in this paper.

References

1. *Safe management of wastes from health-care activities (2014) Second edition, Edited by YvesChartier, Jorge Emmanuel, Ute Pieper, Annette Prüss, Philip Rushbrook, Ruth Stringer, WilliamTownend, Susan Wilburn and Raki Zghondi. World Health Organization. ISBN 978 92 4 1548564.*
2. *IAEA-TECDOC-1183 (2000) Management of radioactive waste from the use of radionuclidesmedicine. Austria: IAEA.*
3. Shoukat K, Syed AT, Reyaz A, et al. (2010) Radioactive waste management in a hospital. *Int JHealth Sci* 4: 39–46.
4. *IAEA-TECDOC-1714 (2013) Management of discharge of low level liquid radioactive wastegenerated in medical, educational, research and industrial facilities. Austria: IAEA.*
5. Sikun Xu G, Chan N (2021) Management of radioactive waste from application of radioactivematerials and small reactors in non-nuclear industries in Canada and the implications for theirnew application in the future. *AIMS Environ Sci* 8: 619–640. doi: 10.3934/environsci.2021039
6. Dawood AMA, Glover ET, Akortia E, et al. (2022) Environmental radiation and health riskassessment in the neighborhood of a radioactive waste management facility. *Environ MonitAssess* 194: 314. <https://doi.org/10.1007/s10661-022-09966-x>
7. Folkers C, Gunter LP (2022) Radioactive releases from the nuclear power sector and implications for child health. *BMJ Paediatr Open* 6: 1–9. <https://doi.org/10.1136/bmjpo-2021-001326>
8. Martínez A, Peñalver T, Baciua M, et al. (2018) Presence of artificial radionuclides in samplesfrom potable water and wastewater treatment plants. *J Environ Rad* 192: 187–193. <https://doi.org/10.1016/j.jenvrad.2018.06.024>
9. Mulas D, Camacho A, Garbayo A, et al. (2019) Medically-derived radionuclides levels in sevenheterogeneous urban wastewater treatment plants: The role of operating conditions andcatchment area. *Sci Total Environ* 663: 818–829. <https://doi.org/10.1016/j.scitotenv.2019.01.349>
10. Teodori F (2021) Health physics calculation framework for environmental impact assessment ofradiological contamination. *AIMS Environ Sci* 8: 403–420.

11. Saeed IMM, Saleh MAM, Hashim S, et al. (2019) Atmospheric dispersion modeling and radiological safety assessment for expected operation of Baiji nuclear power plant potential site. *Ann Nucl Energy* 127: 156–164. <https://doi.org/10.1016/j.anucene.2018.11.045>
12. Chen X, Chen T, Li J, Qiu M, et al. (2019) Ceramic nanofiltration and membrane distillation hybrid membrane processes for the purification and recycling of boric acid from simulated radioactive waste water. *J Membr Sci* 579: 294–301. <https://doi.org/10.1016/j.memsci.2019.02.044>
13. Chugunov A, Vinnitskii, V (2019) Nanofiltration fractionation of radioactive solution components as a method for reducing the volume of wastes intended for permanent disposal. *Nucl Energy Technol* 5: 123–128. <https://doi.org/10.3897/nucet.5.35801>
14. Sancho M, Arnal JM, Verdú-Martín G, et al. (2021) Management of hospital radioactive liquid waste: treatment proposal for radioimmunoassay wastes. *AIMS Environ Sci* 8: 449–464. <https://doi.org/10.3934/environsci.2021029>
15. Guo Z, Chen Y, Lu NL, et al. (2018) Applications of Nanomaterials in Nuclear Waste Management. In *Multifunctional Nanocomposites for Energy and Environmental Applications* (eds Z. Guo, Y. Chen and N.L. Lu).
16. Paraskevoulakos C, Stitt CA, Hallam KR, et al. (2019) Monitoring the degradation of nuclear waste packages induced by interior metallic corrosion using synchrotron X-ray tomography. *Constr Build Mater* 215: 90–103. <https://doi.org/10.1016/j.conbuildmat.2019.04.178>
17. Venkatesan S, Hassan MU, Ryu HJ (2019) Adsorption and immobilization of radioactive ionic-corrosion-products using magnetic hydroxyapatite and cold-sintering for nuclear waste management applications. *J Nucl Mater* 514: 40–49. <https://doi.org/10.1039/c9ra04280f>
18. Romero-Hermida MI, et al. (2020) Environmental Impact of Phosphogypsum-Derived Building Materials. *Int J Environ Res Public Health* 17: 1–17. <https://doi.org/10.3390/ijerph17124248>
19. Natarajan V (2020) A Critical Review on Radioactive Waste Management through Biological Techniques. *Environ Sci Pollut Res Inter* 27: 29812–29823. <https://doi.org/10.1007/s11356-020-08404-0>
20. Giacobbo F, Da Ros M, Macerata E, et al. (2021) A case study of management and disposal of TENORMs: radiological risk estimation by TSD Dose and RESRAD-ONSITE. *AIMS Environ Sci* 8: 465–480. <https://doi.org/10.3934/environsci.2021030>
21. Manobala T, Shukla SK, Rao TS, et al. (2019) Uranium sequestration by biofilm-forming bacteria isolated from marine sediment collected from Southern coastal region of India. *Int Biodeterior Biodegrad* 145: 1–10. <https://doi.org/10.1016/j.ibiod.2019.104809>
22. Mehta N, Benzerara K, Kocar BD, et al. (2019) Sequestration of radionuclides radium-226 and strontium-90 by cyanobacteria forming intracellular calcium carbonates. *Environ Sci Technol* 53: 12639–12647. <https://doi.org/10.1021/acs.est.9b03982>
23. Sun Q, Zhu L, Aguila B, et al. (2019). Optimizing radionuclide sequestration in anion nanotraps with record pertechnetate sorption. *Nat Commun* 10: 1–9. <https://doi.org/10.1038/s41467-019-09630-y>

Evaluation of river water quality in a tropical South Sumatra wetland during COVID-19 pandemic period

**Muhammad Rendana^{1,*}, Yandriani¹, Muhammad Izzudin², Mona Lestari³,
Muhammad Ilham Fattullah¹ and Jimmy Aldian Maulana¹**

¹ Department of Chemical Engineering, Faculty of Engineering, Universitas Sriwijaya, Indralaya
30662 Sumatera Selatan, Indonesia

² Department of of Sociology, Faculty of Social and Political Science, Universitas Sriwijaya,
Indralaya 30662 Sumatera Selatan, Indonesia

³ Department of Public Health Sciences, Faculty of Public Health, Universitas Sriwijaya, Indralaya
30662 Sumatera Selatan, Indonesia

ABSTRACT

The COVID-19 outbreak affected the world badly in this 21st century leading to the closure of all types of anthropogenic activities. It is declared that there was an environmental betterment in names of water quality and air quality during the COVID-19 period. In this study, we analyzed the improvement in water quality by evaluating the suspended particulate matter (SPM) using the remote sensing technique in a tropical South Sumatra wetland i.e., Musi River in Southern Sumatra, Indonesia. The SPM values were estimated from Landsat 8 images Level-2 product. A quantitative and spatial analyses of before (20th May 2019), during (22nd May 2020), and after COVID-19 (28th May 2022) periods were also calculated. Results revealed that the mean SPM values during COVID-19 period (4.56 mg/L) were lower than that before COVID-19 period (8.33 mg/L). Surprisingly, SPM showed an increase of 54% in SPM values after COVID-19 period, compared with during COVID-19 period. The role of human activities including industrial and domestic wastes during the restriction period was the main reason for alteration of pollution loads in the river. Outputs of this study can be used to arrange policies for the sustainable management of aquatic environments and water resources.

Keywords: COVID-19; suspended particulate matter; remote sensing; wetland

Abbreviations:

COVID-19: 2019 novel coronavirus; LSSR: Large scale social restriction; OLI: Operational land imager; SPM: Suspended particulate matter; LEDAPS: Landsat Ecosystem Disturbance Adaptive Processing System; LaSRC: Land Surface Reflectance Code; NTU: Nephelometric Turbidity unit; RMSE: Root means square error; USGS: United States Geological Survey

1. Introduction

Anthropogenic activities are still the main source liable for deteriorating the water quality, although we have seen many actions to preserve susceptible aquatic and terrestrial ecosystems [1]. In Indonesia, it currently produces around 200,000 tons of waste annually, with only 64% reaching landfills while the remaining goes to the surroundings, including aquatic ecosystems [2]. Downs and Piégay [3] found that combining human activities and climate factors had a negative impact on aquatic ecosystems. In-situ measurements are a common method of assessing water quality, but they are timeconsuming and labor-intensive, making it difficult to conduct long-term observations of the aquatic environment [4,5]. Additionally, it calculates only point-to-point information and is not present spatially for the whole water body area [6]. Therefore, the use of remote sensing-based satellite data offers an effective

technique for the rapid and simple study of surface water quality. Remote sensing data provides spatial and temporal information about water quality from local to broad scales [7]. Studies of the quality of water bodies using remote sensing methods have been conducted since the Landsat satellites were introduced.

One of the most prominent water quality parameters is suspended particulate matter (SPM) [8]. The SPM is the most ordinary issue in surface water bodies [9]. These suspended particles decrease the effluence of the sun's light for aquatic species. Furthermore, it is a good benchmark for the eutrophication event [10]. The turbidity of a body of water increases as SPM values in water rise [11]. Several factors can affect the turbidity level due to climate shifts, weather changes, and anthropogenic activities [12,13]. Assessment of suspended matter values from satellite images has become a substantial tool for research to predict and observe suspended sediment variation in bodies of water [14–17]. The turbidity in a body of water is evaluated by how SPM values change water characteristics. It is also found that the SPM values or turbidity exhibit a good association with the visible band of the spectrum, while the red and NIR bands are more susceptible to turbidity [18].

The COVID-19 outbreak has become a lethiferous disease worldwide, affecting more than 200 nations [19]. The COVID-19 pandemic deteriorated many countries and severely affected the global economy [20]. The Indonesian government applied a tight restriction policy (known as large-scale social restriction, LSSR) on April 10, 2020, and this policy led to the closure of offices, mobility, educational places, industries, markets, and social activities [21]. This restriction period was extended into several phases till the whole year 2021, which formed a partial restriction period with a tight COVID-19 protocol. Finally, on May 17, 2022, considering a significant reduction of COVID-19 cases in this country, the Indonesian president announced not to wear a mask in outdoor activities.

Numerous studies have found that decreasing water and air pollution improves global environmental quality [22–25]. In Indonesia, some studies reported that air quality improved during the COVID-19 period [26–29]. However, to date, there have been no studies about how the water quality improved in the Indonesian region during the COVID-19 period. Therefore, it will be a novel study to discuss how water quality conditions in Indonesia. In addition, we chose a unique river within a tropical wetland area, which would be different from other existing studies around the world. To identify whether the decrease in human activities during the COVID-19 period resulted in the improved water quality in the Musi River, South Sumatra, Indonesia, the current study employed remote sensingbased satellite data to analyze alterations in the SPM concentration as a water quality benchmark.

2. Materials and methods

2.1. Study area

The river chosen for the present study is a part of the South Sumatra wetland region, in the province of South Sumatra, Indonesia and lies between 2 57'0"N and 3 0'0"N latitudes and 104 42'0"E–104 51'0"E longitudes (Figure 1).

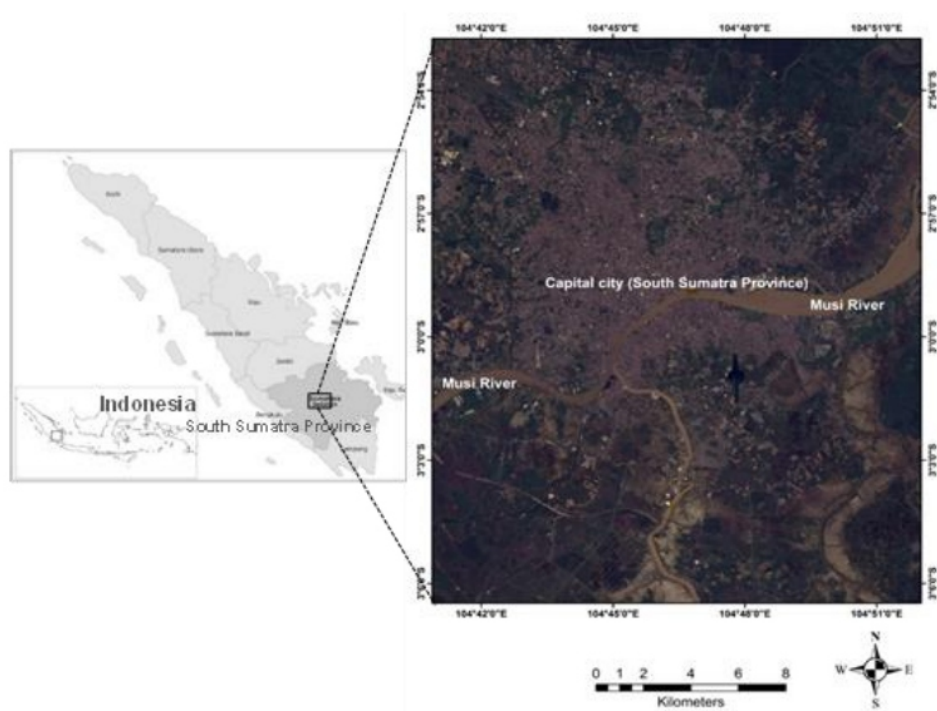


Figure 1. Location of study area.

There are four major kinds of wetlands in South Sumatra, such as tidal swamps, freshwater swamps, lakes, rivers, and peatlands [30]. The Musi River is the primary freshwater contributor to the Musi Estuary. The river flows from southwestern to northeastern, originating from the Barisan Mountains Range that was once a spine of Sumatra Island in Bengkulu Province, to the Bangka Strait and finally flows to the South China Sea. It is approximately 750 km long and becomes the heart of South Sumatra province because it drains most of the South Sumatra region. The water river is used for various needs such as industry, transportation, and households. People used the water for their daily needs, including washing, bathing, and using the restroom directly in the river. Moreover, companies and factories located around the Musi River have contributed to river pollution due to their dumping activities of waste into the river [31]. The annual mean temperature in this region is 24 °C, with the mean annual rainfall of 2,579 mm.

2.2. Data collection and pre-processing stage

In the current study, three Landsat 8 Operational Land Imager (OLI) images of the Musi River area from May 20, 2019 to May 28, 2022 were obtained from the United States Geological Survey (USGS). Table 1 showed the specification of the Landsat 8 satellite images that used in this study. We used the month of May because the COVID-19 restriction policy in the study area was started in that month thus to reduce the bias in selecting the other months, we chose the same month for all periods of study. In this study, all the satellite images downloaded were of level-2 type, meaning that they had a major improvement in the absolute geo-location accuracy of the global ground reference dataset, which enhanced the interoperability of the Landsat archive over time. This level-2 type has also been updated with global digital elevation modeling sources and validation updates. Surface reflectance is used to quantify the proportion of incoming solar radiation that is thrown from the surface of the earth to the Landsat sensor. The Landsat Ecosystem Disturbance Adaptive Processing System (LEDAPS) and Land Surface Reflectance Code (LaSRC) surface reflectance algorithms compensate for the spectral, spatial, and

temporal effects of atmospheric aerosols, gaseous, and water vapor, which are required to analyze the earth's land surface. Therefore, to obtain surface reflectance values from Landsat 8 level-2 type images, we used a scale factor of 0.0000275 and an additional offset of −0.2 per pixel.

Table 1. Specifications of the Landsat 8 satellite images and the study period.

Product ID	Band used	RMSE	%Cloud	Period
LC08_L2SP_124062_20190520_20200828_02_T1	Band 4 (0.630 to 0.680 μm)	0.087	9.20	2019 (before COVID-19 period)
LC08_L2SP_124062_20200522_20200820_02_T1	Band 4 (0.630 to 0.680 μm)	0.056	8.05	2020 (During COVID-19 period)
LC08_L2SP_124062_20220528_20220603_02_T1	Band 4 (0.630 to 0.680 μm)	0.030	7.56	2022 (After COVID-19 period)

2.3. Suspended particulate matter (SPM) calculation

Based on a prior study, Fachrurrozi [31] measured the turbidity value of the Musi River and reported it varied from 7 to 9 NTU. The NTU is the acronym of Nephelometric Turbidity unit. The specific unit used to gauge the turbidity of water or the suspended matters in water. Furthermore, Trisnaini et al. [32] measured turbidity values in the Musi River around dense areas and found them to be lower than 50 NTU. These studies stated that the turbidity value in the Musi River is below 110 mg/L. Several studies have explained that using a single band for turbidity analysis can obtain a good result if the band is selected in the right way [33,34]. Therefore, the current study applied a SPM algorithm to evaluate the SPM values for water, and it showed good performance when the SPM values were less than 110 mg/L [35]. The SPM is computed by using the red band based on Eq (1) below:

$$\text{SPM} = \frac{A \rho_w}{(1 - \rho_w)/B} \quad (1)$$

where A and B are empirical constants: and A = 289.29 and B = 0.1686. ρ_w is water-leaving reflectance from the red band (655 nm). The empirical constant of A came from the previous study by Nechad et al. [35] that found this value (A = 289.29) gave the best fit to total suspended matter and the subsurface reflectance calculations. While, the empirical constant of B was set to 0.1686 because the satellite sensor and its process would possibly have dissimilar measurement errors from the data calibration. A higher SPM value from the Eq 1 showed more turbid water or dirty water, while the lower SPM value indicated cleaner water. Our study found there was a high association between the SPM and the band ratio of the water-leaving radiances at 655 nm (Figure 2). It could be concluded that the model showed a good performance, with the R-squared of 0.95, the RMSE of 15% and the standard deviation of 2.5mg/L. The accuracy assessment of this study was carried out using the Pearson's correlation between the satellite-based SPM data and the in-situ SPM measurement. Thus, we have applied the Pearson's correlation coefficient (R²), mean absolute error (MAE), and root means square error (RMSE) analyses in this study. Our finding obtained the values of R² was 0.92, MAE was 0.04, and RMSE was 0.08, indicating a good accuracy.

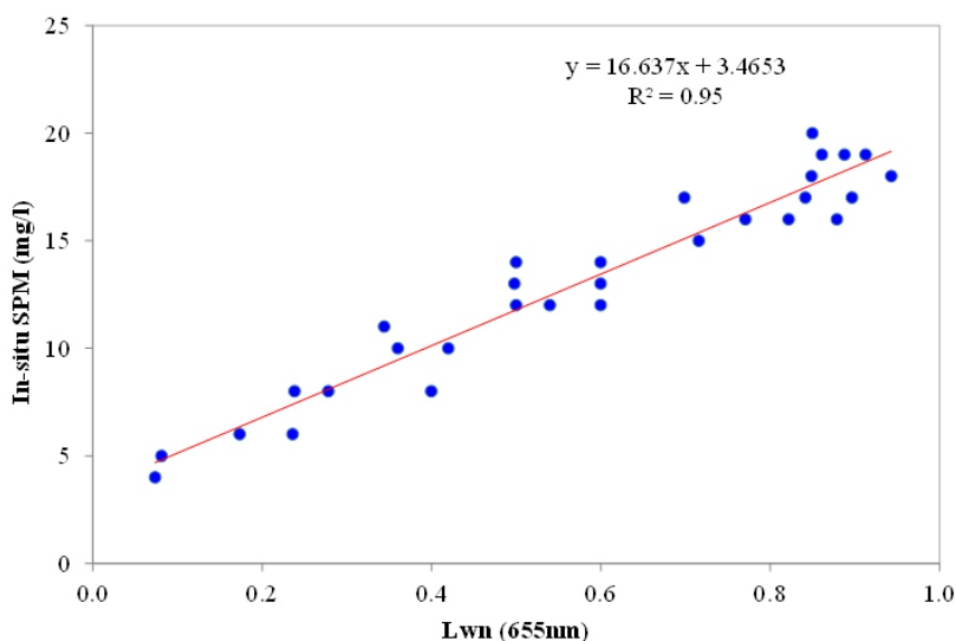


Figure 2. The association between the field-measured SPM concentration and the band ratio of the water-leaving radiance at 655 nm.

3. Results and discussion

The spatial and temporal distribution of SPM values in the Musi River from 2019 to 2022, including before, during, and after COVID-19 periods, was depicted in Figure 3. It could be observed that a reduction in SPM values during the COVID-19 period was found compared to before the COVID-19 period. The dense urban area that mostly located at the middle and downstream areas led to higher number of pollutants entried into the river due to domestic and industrial activities (Figure 3(a)). During the COVID-19 period, the upstream area showed higher SPM values than the downstream area. It might be due to the natural process such as soil erosion at the upstream area. The higher altitude of the upstream area contributed to high risk of soil erosion and especially during the rainfall. In contrast, the downstream area sustained a great reduction due to anthropogenic activities restriction (Figure 3(b)). After the COVID-19 period, the SPM values started to rebound at the same level at before the COVID-19 period, it was shown by the SPM values from the middle to downstream areas gradually increased (Figure 3©).

To analyze further the reduction in SPM concentrations of the Musi River, we analyzed the situation of the river around the busy port area before and during the COVID-19 periods using Sentinel 2 data (Figures 4(a),(b)). The result found there was a decrease in vessel traffic along the Musi River. The number of black vessels that carried coal products has been reduced, as have the white vessels that are commonly used as public transport for people. Traffic condition along the Musi River near the main port. Due to the low number of vessels sailed along the Musi River, it would certainly diminish the total discharge of the water pollutants originating from the vessels into the river. This result was consistent with other studies [36].

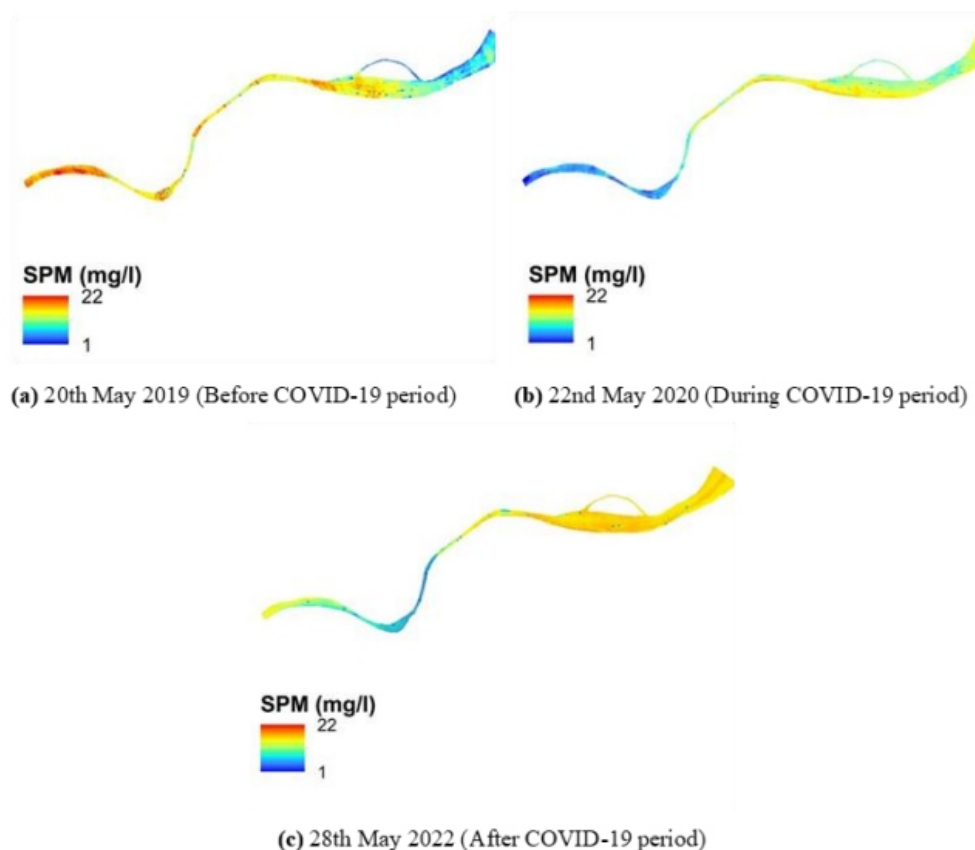


Figure 3. Changes in SPM values predicted for the Musi River from 20th May 2019 to 28th May 2022. Red color shows higher values of SPM while blue color shows low values.

Effects of inter-monthly and rainfall factors could also contribute to decreases in SPM values, as stated in a study by Moquet et al. [37]. Time series Landsat 8 images from different years but in the same month were chosen, and precipitation data were also evaluated and obtained, no significant difference was found during the study period. This showed that the COVID-19 restriction policy (largescale social restriction policy) has greatly affected the water quality of the Musi River and significantly reduced the pollution level. Furthermore, the pollution from industrial sources, domestic sources, and other related human activities was less during the COVID-19 restriction policy, and thus it improved the water quality of the river.



(a). Before COVID-19 period (in May 2019).



(b). During COVID-19 period (in May 2020).

Figure 4 Traffic condition along the Musi River near the main port. Black vessels: coal transport, white vessels: public transport.

A comparison of the SPM values in the Musi River in several study periods was tabulated in Table 2. Our results revealed that the highest average SPM values of 8.33 mg/L were observed in May 2019, followed by 2022 (7.06 mg/L) and 2020 (4.56 mg/L). It was recorded that SPM values during the COVID-19 period varied from 1 mg/L to 11 mg/L with an average SPM of 4.56 mg/L, which was lower than before the COVID-19 period. Furthermore, a comparison between the pre-COVID-19 period and the COVID-19 period obtained a reduction of the total average SPM concentration from 8.33 mg/L to 4.56 mg/L (Table 2).

Spatial analysis exhibited that higher SPM values were found in the southwestern area (the most congested areas in the South Sumatra Region). Specifically, this occurred during the year 2019 and then this SPM was decreased during the COVID-19 period in 2020, where this spatial pattern was more concentrated in the northeastern area. We assumed the lower SPM value in the northeastern region during the COVID-19 period, as compared with before the COVID-19 period, might be due to the application of the COVID-19 restriction policy. This might be due to the fact that since it was near to industrial areas, the COVID-19 period resulted in the closure of industrial activities, thus the pollution levels decreased in those areas. A quantitative analysis between mean SPM values of the preCOVID-19

period and SPM values during the COVID-19 period in the northeastern regions showed a notable reduction in SPM concentrations during the COVID-19 period as compared with the pre COVID-19 period (Figure 2(a),(b)). In the COVID-19 period, which in this study we took two years interval, we found a substantial increase in SPM concentration of about 54%, as compared with the COVID-19 period (Figure 2©). The changes of SPM also associated with other water quality parameters like Cu, As, Fe and Ni metals. It was because the heavy metals were transported together with organic or sediment masses. Suspended sediments brought metals into river flow through runoff event. Surface sediments carried metals from anthropogenic sources into the river. A previous study by Rahutami et al. [38] found there was a linear increase between the SPM with Fe, Cr, and Pb concentrations in the Musi river.

Table 2. SPM values of the Musi River for the study periods.

Date of satellite images	SPM values				Notes
	Min	Max	Average	SD	
20/05/2019	2.67	10.50	7.06	0.71	Before COVID-19 period
22/05/2020	1.03	11.19	4.56	0.67	During COVID-19 period
28/05/2022	3.03	21.83	8.33	1.31	After COVID-19 period

Additionally, heavy metals in water mostly accumulated in the SPM due to direct contact with the water and the precipitation of metal-absorbed [39]. Thus, the SPM is the main process for the deposition of heavy metals in floor sediments. This is a prominent process for the understanding of heavy metals in the water-sediment interface. A study by Helali et al. [40] in the Gulf of Tunis found that heavy metals (Cu, Pb, Fe, and Zn) were primarily caused by commercial and fishing activities. In the Musi river, a previous study by Tjahjono et al. [41] has found that Pb concentration in the water could be associated with the SPM value. The highest SPM value was found in the busy port around the Musi river where the Pb content has exceeded the water quality standard (0.03 mg/L). The concentration of Pb in the water showed that the presence of oil spills due to water activities. Furthermore, the Cd concentration in the Musi river was constant but it still exceeded the quality standard (0.01 mg/L). The high Cd concentration was due to the excessive use of fertilizers around the basin. The correlation analysis based on this study showed a weak correlation between both metals and SPM. But, in another study by Wang et al. [42] which located in the Huanghe River, China, they found a high significant correlation between Pb and SPM ($r = 0.84$, $p < 0.01$). It could be assumed that when the SPM was high, dissolved metals were prone to be scavenged via aggregating into compact particles, thus dissolved metals reduced to the sea [43].

Although this study showed lower SPM values than before the COVID-19 period in 2019, there was an increase in the pollution level during that period. This might be due to the fact that the withdrawal of restriction policies in social activities, industrial and commercial sectors has allowed the intrusion of waste into the lake, which changed the pollution loads in the Musi River. Therefore, the restriction of human activities such as commercial and industries has contributed to the reduction of SPM value in the Musi River. Due to the restriction policy and lack of in-situ data, the validation with in-situ data was not carried out in this current work. But our results were comparable with the other studies carried out in Indonesian regions. Because there was a lack of studies in our region discussing the SPM changes during the COVID-19 period, we compared our results with other studies outside the country. For instance, Yunus et al. [44] analyzed the SPM level changes during the lockdown period in Vembanad lake, India and found a 15.9% decrease in SPM compared to before the lockdown period. Another study

by Liu et al. [13] also revealed the SPM changes in Min River, China and reported a 48% decrease in SPM. Those above-mentioned results were the same as the outputs of our study. In contrast, Tokatlı and Varol [45] analyzed the water quality changes in the Meriç-Ergene River Basin, Turkey and found no significant differences between before the lockdown and during lockdown periods. This might be due to nonstop agricultural activities and domestic wastewater discharges into the water body during the lockdown period. The agricultural wastes (organic and chemical fertilizers) were the main effluents in the river which located near agricultural areas [46].

Hence, the COVID-19 restriction not only resulted in an increase in water quality but also an improvement in air quality [47]. Several studies revealed air quality parameters such as PM_{2.5}, PM₁₀, SO₂, NO₂, and CO showed major reductions that led to an improvement in the air quality index during lockdown period in Tehran [48], China [49] and Germany [50]. The lower SPM concentrations in the South Sumatera wetland helped to improve the sun light effluence and surely had positive effects on freshwater ecosystems and the environmental condition of the water body. For future studies, the data was extracted from satellite only, and thus it might be hard to obtain accurate data on the physical and chemical properties. Hence, in situ fieldwork was needed to arrange an appropriate management policy to face the COVID-19 pandemic period. Therefore, a study was done to analyze the spatial and temporal data on water quality of the South Sumatera wetland. Despite other human activity factors, the COVID-19 restriction policy in this study area was likely to start a recovery process for the ecosystem. But authorities should give more attention to the alteration of river pollution, which is how this restriction has affected water bodies. Therefore, it was also recommended that this policy could increase the self-recovery of the ecosystems.

4. Conclusions

COVID-19 has become a serious threat to our lives, with more than 150 million people infected and around 3 million deaths announced all over the world in May 2021. Due to the large transmission of COVID-19, many nations implemented a total lockdown with full restrictions on social, economic, industrial, spiritual, schools, and other activities. But on the other hand, this restriction successfully had a good impact on the environment by decreasing air and water pollution. In this recent study, we tried to analyze the impact of the COVID-19 period on the Musi River by using remote sensing and GIS techniques. Even though we could not determine the particular origins of river pollution, the output of this study revealed that water quality (SPM as an indicator) could improve significantly as human activities were diminished. The analysis of the SPM value in Musi River using Landsat 8 images revealed that SPM values during the COVID-19 period (average SPM of 4.56 mg/L) were lower than before the COVID-19 period (8.33 mg/L) and the next two years (average of 7.06 mg/L). Mean reduction of 45% was reported in SPM values during the COVID-19 period compared to before the COVID-19 period. It was also found that after the COVID-19 period with the loosening restriction policy, domestic waste started to enter the Musi River again, which, followed by industrial waste, were the main activities that aggravated the water pollution in the Musi River. As a result, the current study provided important insights into the future management of the Musi River and other wetland and aquatic environments. In addition, the authorities should know about the improved water quality due to the decreased human activities and should arrange an effective action plan for the future Musi River management policy.

Acknowledgments

This research is an additional output of the research grant that is funded by PNBP, Faculty of Engineering, Universitas Sriwijaya, year 2021 SP DIPA-023.17.2.677515/2022 on November 17,

2021, In accordance with Rector's Decree Number: 0390/UN9.FT/TU.SK/2022, on May 13, 2022.

Conflict of interest

Conflict of interest on behalf of all authors. The corresponding author states that there is no conflict of interest.

References

1. Hoang HTT, Duong TT, Nguyen KT, et al. (2018) *Impact of anthropogenic activities on water quality and plankton communities in the Day River (Red River Delta, Vietnam)*. *Environ Monit Assess* 190: 67. <https://doi.org/10.1007/s10661-017-6435-z>
2. Indonesian Ministry of Environment and Forestry, *Gembira Bersama Kelola Sampah Menuju Hidup Bersih Dan Sehat*, 2018. Available from: <http://www.menlhk.go.id/berita-403-gembira-bersama-kelola-sampah-menuju-hidup-bersih-dan-sehat.html>.
3. Downs PW, Piégay H (2019) *Catchment-scale cumulative impact of human activities on river channels in the late Anthropocene: Implications, limitations, prospect*. *Geomorphology* 338: 88–104. <https://doi.org/10.1016/j.geomorph.2019.03.021>
4. Ahmed AN, Othman FB, Afan HA, et al. (2019) *Machine learning methods for better water quality prediction*. *J Hydrol* 578: 124084. <https://doi.org/10.1016/j.jhydrol.2019.124084>
5. Tung TM, Yaseen ZM (2020) *A survey on river water quality modelling using artificial intelligence models: 2000–2020*. *J Hydrol* 585: 124670. <https://doi.org/10.1016/j.jhydrol.2020.124670>
6. He Y, Jin SG, Shang W (2021) *Water quality variability and related factors along the Yangtze River using Landsat-8*. *Remote Sens* 13: 2241. <https://doi.org/10.3390/rs13122241>
7. Kasampalis DA, Alexandridis TK, Deva C, et al. (2018) *Contribution of remote sensing on crop models: A review*. *J Imaging* 4: 52. <https://doi.org/10.3390/jimaging4040052>
8. Chakraborty B, Roy S, Bera A, et al. (2021) *Eco-restoration of river water quality during COVID19 lockdown in the industrial belt of eastern India*. *Environ Sci Pollut Res* 28: 25514–25528. <https://doi.org/10.1007/s11356-021-12461-4>
9. Elhag M, Gitas I, Othman A, et al. (2019) *Assessment of water quality parameters using temporal remote sensing spectral reflectance in arid environments, Saudi Arabia*. *Water* 11: 556. <https://doi.org/10.3390/w11030556>
10. Yang P, Yang CH, Yin HB (2020) *Dynamics of phosphorus composition in suspended particulate matter from a turbid eutrophic shallow lake (Lake Chaohu, China): Implications for phosphorus cycling and management*. *Sci Total Environ* 741: 140203. <https://doi.org/10.1016/j.scitotenv.2020.140203>
11. Tavora J, Fernandes EHL, Thomas AC, et al. (2019) *The influence of river discharge and wind on Patos Lagoon, Brazil, Suspended Particulate Matter*. *Int J Remote Sens* 40: 4506–4525. <https://doi.org/10.1080/01431161.2019.1569279>
12. Martins VS, Kaleita A, Barbosa CCF, et al. (2019) *Remote sensing of large reservoir in the drought years: Implications on surface water change and turbidity variability of Sobradinho reservoir (Northeast Brazil)*. *Remote Sens Appl: Soc Environ* 13: 275–288. <https://doi.org/10.1016/j.rsase.2018.11.006>
13. Liu H, Zhou W, Li XW, et al. (2020) *How many submerged macrophyte species are needed to improve water clarity and quality in Yangtze floodplain lakes?* *Sci Total Environ* 724: 138267. <https://doi.org/10.1016/j.scitotenv.2020.138267>
14. Tsapanou A, Oikonomou E, Drakopoulos P, et al. (2020) *Coupling remote sensing data with insitu optical measurements to estimate suspended particulate matter under the Evros river influence (North-*

- East Aegean sea, Greece*). *Int J Remote Sens* 41: 2062–2080. <https://doi.org/10.1080/01431161.2019.1685713>
15. Li P, Ke YH, Wang DW, et al. (2021) Human impact on suspended particulate matter in the Yellow River Estuary, China: Evidence from remote sensing data fusion using an improved spatiotemporal fusion method. *Sci Total Environ* 750: 141612. <https://doi.org/10.1016/j.scitotenv.2020.141612>
 16. Lavrova OY, Nazirova KR, Soloviev DM, et al. (2021) Remote sensing of suspended particulate matter: Case studies of the Sulak (Caspian Sea) and the Mzymta (Black Sea) mouth areas, *Remote Sensing of the Ocean, Sea Ice, Coastal Waters, and Large Water Regions* 2021 11857: 1185705. <https://doi.org/10.1117/12.2599809>
 17. Vanhellemont Q, Ruddick K (2021) Atmospheric correction of Sentinel-3/OLCI data for mapping of suspended particulate matter and chlorophyll-a concentration in Belgian turbid coastal waters. *Remote Sens Environ* 256: 112284. <https://doi.org/10.1016/j.rse.2021.112284>
 18. Xu HQ, Xu GZ, Wen XL, et al. (2021) Lockdown effects on total suspended solids concentrations in the Lower Min River (China) during COVID-19 using time-series remote sensing images. *Int J Appl Earth Obs* 98: 102301. <https://doi.org/10.1016/j.jag.2021.102301>
 19. Ahmed N, Maqsood A, Abduljabbar T, et al. (2020) Tobacco smoking a potential risk factor in transmission of COVID-19 infection. *Pak J Med Sci* 36: S104–107.
 20. Rendana M., Idris WMR, Abd Rahim S (2022) Effect of COVID-19 movement control order policy on water quality changes in Sungai Langat, Selangor, Malaysia within distinct land use areas. *Sains Malays* 51: 1587–1598.
 21. Rendana M, Idris WMR, Rahim SA (2022) Changes in air quality during and after large-scale social restriction periods in Jakarta city, Indonesia. *Acta Geophys* 70: 2161–2169. <https://doi.org/10.1007/s11600-022-00873-w>
 22. Dutta V, Dubey D, Kumar S (2020) Cleaning the River Ganga: Impact of lockdown on water quality and future implications on river rejuvenation strategies. *Sci Total Environ* 743: 140756. <https://doi.org/10.1016/j.scitotenv.2020.140756>
 23. Resmi CT, Nishanth T, Kumar MKS, et al. (2020) Air quality improvement during triple lockdown in the coastal city of Kannur, Kerala to combat Covid-19 transmission. *PeerJ* 8: e9642.
 24. Chakraborty S, Sarkar K, Chakraborty S, et al. (2021) Assessment of the surface water quality improvement during pandemic lockdown in ecologically stressed Hooghly River (Ganges) Estuary, West Bengal, India. *Mar Pollut Bull* 171: 112711. <https://doi.org/10.1016/j.marpolbul.2021.112711>
 25. Pal SC, Chowdhuri I, Saha A, et al. (2021) Improvement in ambient-air-quality reduced temperature during the COVID-19 lockdown period in India. *Environ Dev Sustain* 23: 9581–9608. <https://doi.org/10.1007/s10668-020-01034-z>
 26. Anugerah AR, Muttaqin PS, Purnama DA (2021) Effect of large-scale social restriction (PSBB) during COVID-19 on outdoor air quality: Evidence from five cities in DKI Jakarta Province, Indonesia. *Environ Res* 197: 111164. <https://doi.org/10.1016/j.envres.2021.111164>
 27. Rahutomo R, Purwandari K, Sigalingging JWC, et al. (2021) Improvement of Jakarta's air quality during large scale social restriction, *IOP Conf Ser: Earth Environ Sci* 729: 12132. <https://doi.org/10.1088/1755-1315/729/1/012132>
 28. Jakob A, Hasibuan S, Fiantis D (2022) Empirical evidence shows that air quality changes during COVID-19 pandemic lockdown in Jakarta, Indonesia are due to seasonal variation, not restricted movements. *Environ Res* 208: 112391. <https://doi.org/10.1016/j.envres.2021.112391>
 29. Santoso M, Hopke PK, Permadi DA, et al. (2021) Multiple air quality monitoring evidence of the impacts of large-scale social restrictions during the COVID-19 pandemic in Jakarta, Indonesia. *Aerosol Air Qual Res* 21: 200645.

30. Armanto M, Wildayana E, Syakina B (2018) *Similarity prosiding: Dynamics, degradation and future challenges of wetlands in South Sumatra province, Indonesia*, E3S Web of Conferences.
31. Fachrurrozi M (2017) *Real time monitoring system of pollution waste on Musi River using Support Vector Machine (SVM) method*, IOP Conf Ser: Mater Sci Eng 190: 012014.
32. Trisnaini I, Faisya AF, Idris H (2020) *Spatial analysis of water quality in area of the riverbank of Musi River in Palembang City*, 2nd Sriwijaya International Conference of Public Health (SICPH 2019), 110–120. <https://doi.org/10.2991/ahsr.k.200612.014>
33. Lee CM, Hestir EL, Tuffillaro N, et al. (2021) *Monitoring turbidity in San Francisco Estuary and Sacramento–San Joaquin delta using satellite remote sensing*. JAWRA 57: 737–751. <https://doi.org/10.1111/1752-1688.12917>
34. Heltria S, Nurjaya IW, Gaol JL (2021) *Turbidity front dynamics of the Musi Banyuasin Estuary using numerical model and Landsat 8 satellite*. AACL Bioflux 14: 1–13.
35. Nechad B, Ruddick KG, Park Yjrs (2010) *Calibration and validation of a generic multisensor algorithm for mapping of total suspended matter in turbid waters*. Remote Sens Environ 114: 854–866. <https://doi.org/10.1016/j.rse.2009.11.022>
36. March D, Metcalfe K, Tintoré J, et al. (2021) *Tracking the global reduction of marine traffic during the COVID-19 pandemic*. Nat Commun 12: 2415. <https://doi.org/10.1038/s41467-021-22423-6>
37. Moquet J-S, Morera S, Turcq B, et al. (2020) *Control of seasonal and inter-annual rainfall distribution on the Strontium-Neodymium isotopic compositions of suspended particulate matter and implications for tracing ENSO events in the Pacific coast (Tumbes basin, Peru)*. Global Planet Change 185: 103080. <https://doi.org/10.1016/j.gloplacha.2019.103080>
38. Rahutami S, Said M, Ibrahim E, et al. (2022) *Actual status assessment and prediction of the Musi River water quality, Palembang, South Sumatra, Indonesia*. J Ecol Eng 23: 68–79.
39. Zeng J, Han GL, Yang KH (2020) *Assessment and sources of heavy metals in suspended particulate matter in a tropical catchment, northeast Thailand*. J Clean Prod 265: 121898. <https://doi.org/10.1016/j.jclepro.2020.121898>
40. Helali MA, Oueslati W, Zaaboub N, et al. (2016) *Chemical speciation of Fe, Mn, Pb, Zn, cd, cu, co, Ni and Cr in the suspended particulate matter off the Mejerda River Delta (gulf of Tunis, Tunisia)*. J Afr Earth Sci 118: 35–44. <https://doi.org/10.1016/j.jafrearsci.2016.02.013>
41. Tjahjono A, Sugiharto R, Wahyuni O (2022) *Study of water and sediment surface quality on defilement of heavy metals Pb & Cd at a downstream section of Musi River, South Sumatera, Indonesia*. Rev Ambient Agua 17: e2799. <https://doi.org/10.4136/ambi-agua.2799>
42. Wang Y, Liu RH, Zhang YQ, et al. (2016) *Transport of heavy metals in the Huanghe River estuary, China*. Environ Earth Sci 75: 288. <https://doi.org/10.1007/s12665-015-4908-3>
43. Zhang YY, Zhang ER, Zhang J (2008) *Modeling on adsorption–desorption of trace metals to suspended particle matter in the Changjiang Estuary*. Environ Geol 53: 1751–1766. <https://doi.org/10.1007/s00254-007-0781-z>
44. Yunus AP, Masago Y, Hijioka Y (2020) *COVID-19 and surface water quality: Improved lake water quality during the lockdown*. Sci Total Environ 731: 139012. <https://doi.org/10.1016/j.scitotenv.2020.139012>
45. Tokath C, Varol M (2021) *Impact of the COVID-19 lockdown period on surface water quality in the Meriç-Ergene River Basin, Northwest Turkey*. Environ Res 197: 111051. <https://doi.org/10.1016/j.envres.2021.111051>
46. Rendana M, Rahim SA, Idris WMR, et al. (2016) *Mapping nutrient status in oil palm plantation using geographic information system*. Asian J Agric Res 10: 144–153.
47. Rendana M, Idris WMR, Rahim SA (2021). *Spatial distribution of COVID-19 cases, epidemic*

spread rate, spatial pattern, and its correlation with meteorological factors during the first to the second waves. *J Infect Public Heal* 14: 1340–13

48. <https://doi.org/10.1016/j.jiph.2021.07.01048>. Wang MC, Liu F, Zheng MN (2021) Air quality improvement from COVID-19 lockdown: Evidence from China. *Air Qual Atmos Health* 14: 591–604. <https://doi.org/10.1007/s11869-020-00963-y>

49. Fuladlu K, Altan H (2021) Examining land surface temperature and relations with the major air pollutants: A remote sensing research in case of Tehran. *Urban Clim* 39: 100958. <https://doi.org/10.1016/j.uclim.2021.100958>

50. Fuladlu K, Altan H (2022) Examination of the population density impact on major air pollutants: A study in the case of Germany, In: *Innovating strategies and solutions for urban performance and regeneration*, Cham: Springer, 211–218.

Soil erosion estimation using Erosion Potential Method in the Vjosa River Basin, Albania

Oltion Marko¹, Joana Gjipalaj^{1,*}, Dritan Profka¹ and Neritan Shkodrani²

¹ Department of Environmental Engineering, Faculty of Civil Engineering, Polytechnic University of Tirana, Rruga Muhamet Gjolllesha Nr. 54, 1023, Tirana, Albania

² Department of Civil Engineering, Faculty of Civil Engineering, Polytechnic University of Tirana, Rruga Muhamet Gjolllesha Nr. 54, 1023, Tirana, Albania

ABSTRACT

Soil erosion is a major environmental threat to soil sustainability and productivity with knock-on effects on agriculture, climate change, etc. Factors influencing soil erosion are many and usually divided into natural and human causes. Massive deforestation, intensive agriculture, temperature and wind, rainfall intensity, human activities and climate changes are listed as the main causes of soil erosion. Calculation of the coefficient of soil erosion is very important to prevent the event. One of the methods used worldwide to calculate soil loss and the erosion coefficient is the Erosion Potential Method. In this study, 49 sub-basins of the Vjosa River Basin in Albania were evaluated. Results showed that the phenomenon of erosion is present in all sub-basins, varying from 0.01 to 0.71. Thus, the categorization of soil erosion varies from heavy to very slight erosion. Moreover, the overall sediment yield calculated for the Vjosa River Basin was 2326917 m³/year. In conclusion, the application of the Erosion Potential Method is reliable for evaluating erosion and can further be applied in our country's conditions.

Keywords: *soil erosion; Vjosa River Basin; Erosion Potential Method (EPM); sediment yield; Albania*

1. Introduction

The concept of erosion is commonly considered as the displacement and transportation of various portions of the land [1]. The advancement of soil erosion is mainly dependent on natural and human factors, such as rainfall, temperature changes, wind, land use and climate changes [2–9]. Soil erosion is defined as slow, high or even very high when conditions causing it are very consistent. Moreover, other human activities, such as large deforestation, intensive use of agricultural land and the increasing population worldwide, are considered as events affecting soil erosion. Larger volumes of materials involved in the erosion process can cause major damages since these materials can travel long distances, causing the pollution of water bodies in terms of nutrients [10–15]. Likewise, flow rates can be influenced by these events when they settle down at one final point. Since the land degradation process is a very complex occurrence that is difficult to predict, the generation of maps showing land erosion and sediment yield is considered a very significant step to oppose the process. Many authorities and authors have been proposing different methods to evaluate sediment yield and soil erosion. Several models have been developed, including the universal Soil Loss Equation (USLE) [16], Revised Universal Soil Loss Equation (RUSLE) [17], Modified Universal Soil Loss Equation (MUSLE) [18] and Erosion Potential Method (EPM) [19].

The EPM estimates the amount of sediment production and transportation, thus indicating the zones potentially threatened by erosion. This method was first used by Gavrilovic in the former Yugoslavia.

The method itself is a semi quantitative method that is applied in many countries [20–25], especially in the Balkans, to evaluate the erosion mainly in semi-arid and arid areas [26–33]. In our country's conditions, erosion of lands is consistent, especially in specific districts [34].

Furthermore, few studies have been done in Albania using the Erosion Potential Method to estimate erosion [26]. We assume that application of such methodology can help in identifying the zones with a high erosion rate, in order to prevent the phenomenon's progression.

2. Materials and methods

2.1. Study area

The Vjosa River basin (VRB) is the second largest river basin in Albania (6474 km²), drained by the Vjosa River (Figure 1a). The Vjosa river is one of the last wild and free flowing rivers in Europe [35]. Moreover, the Vjosa River is one of the longest (272 km) transboundary rivers in the Balkan area. It flows from its source in the Pindos mountains in Greece through the south of Albania until its discharge in the Adriatic Sea. One third of it (80 km) is located in northwest Greece, where it is known as the Aoös (Αώος) River; and the other part is in Albania, where it continues as the Vjosa River and flows over a distance of 192 km before discharging into the Adriatic Sea north of the Narta Lagoon. The most important tributaries of the Vjosa River in Albania are the Drino, Bënça and Shushica. The Vjosa River Basin is configured in 49 sub-basins (Figure 1b), has a mean elevation of about 855 m above sea level and has a perimeter of about 906.13 km. Due to the large perimeter and surface of the Vjosa River Basin, its territory includes natural, agricultural and urban spaces.

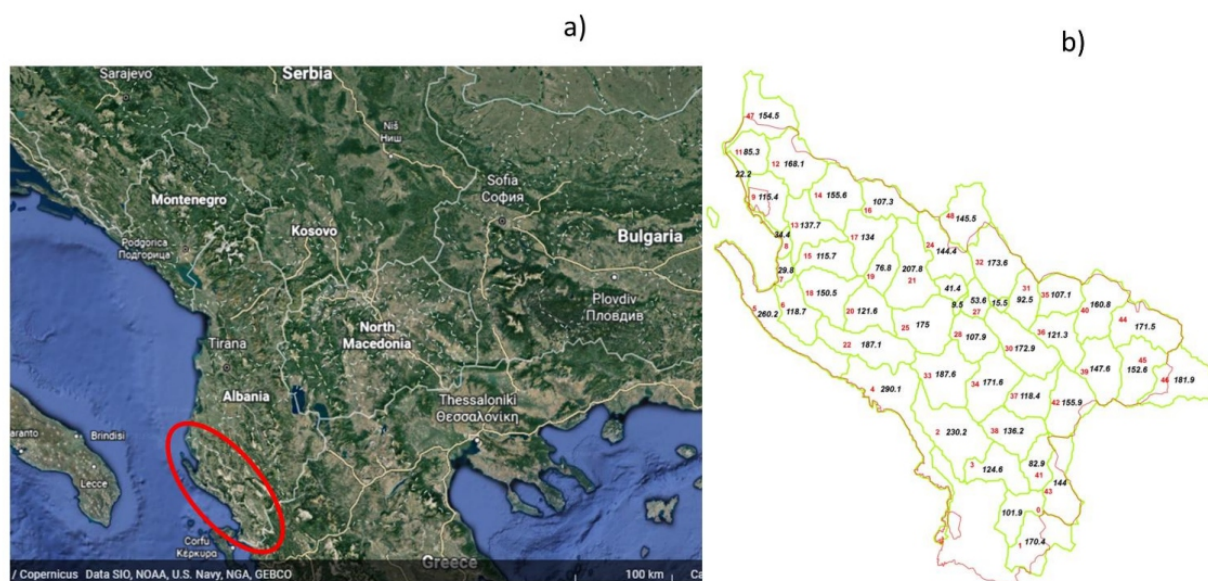


Figure 1. Location of Vjosa River Basin, Albania (a) (source: Google Earth); sub-basin divisions (b).

2.2. Description of erosion potential method

EPM is a widely known methodology first designed by Gavrilovic [19] for the estimation of erosion coefficient and for the evaluation of sediment production and transportation.

The methodology was used for the first time in the Balkan area (Serbia and Croatia), followed by studies conducted all over Europe and worldwide [20–24, 26–33]. According to the original description of the method, for the Vjosa River Basin, the following parameters were calculated: the annual volume of soil loss W_a (Eq 1), the temperature coefficient T (Eq 2), the erosion coefficient Z (Eq 3), the actual

sediment yield G (Eq 4) and the sediment delivery ratio D_r (Eq 5). Moreover, the specific eroded sediment E per sub-basin of the Vjosa River Basin was calculated as a report of the eroded material and the surface of the sub-basin, expressed in ha. For the assessment of parameters used in Eq 3, the land use coefficient, soil erodibility and active erosion processes, the classification was based on the Zemljic classification system [36]. Equations, followed by detailed description of the data set used to evaluate the Erosion Potential Method, are shown in Table 1.

Table 1. Equations and descriptive variables used in the Erosion Potential Model (EPM).

Equation	Parameter descriptions
1 $W_a = \pi \times S \times T \times h \times \sqrt{Z^3}$	W - the annual volume of soil loss (m ³ /year) S - the sub-basin area (km ²) T - the temperature coefficient (-) h - the mean annual precipitation (mm) Z - the erosion coefficient (-)
2 $T = \sqrt{\frac{t}{10}} + 0.1$	t - the mean annual temperature (°C)
3 $Z = x \times y \times (\varphi + \sqrt{i_m})$	x - land cover coefficient y - soil erodibility φ - active erosion processes i_m - the mean slope (%)
4 $G = W \times D_r$	G - the real sediment production (m ³ /year) D_r - the sediment delivery ratio (-)
5 $D_r = \frac{\sqrt{H \times P}}{0.25 \times (L + 10)}$	H - the mean height distance of the basin (km) P - the perimeter of the basin (km) L - the length of the basin (km)

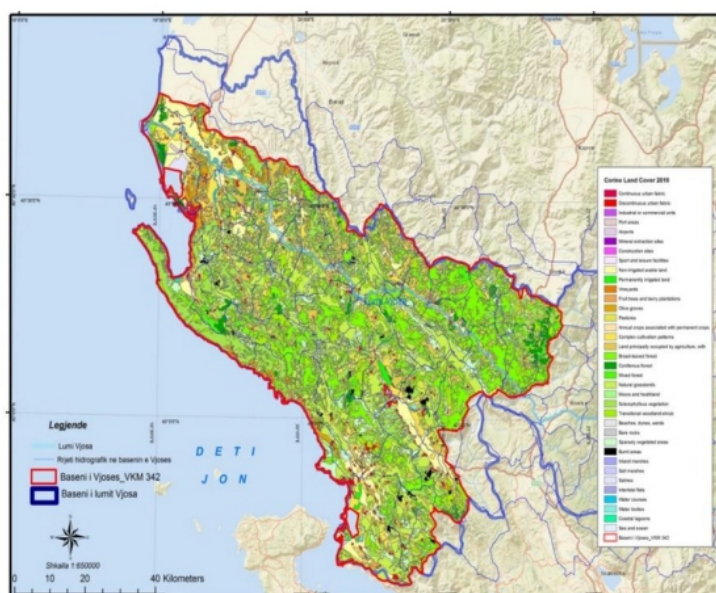
The application of the Erosion Potential Method was based on data gathered from different field surveys and satellite sources, given in Table 2.

Coefficient of soil erodibility y for each sub-basin was determined using the geological maps of 2021 with a scale of 1:650000 (Figure 2) of the Albanian Geological Service, as shown in Table 2.

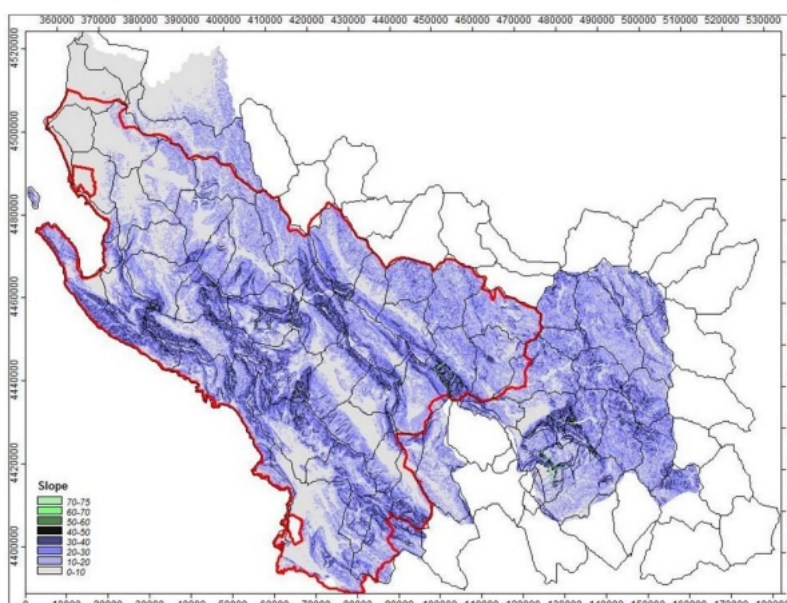


Figure 2. Geological map of the Vjosa River Basin, Albania.

For the evaluation of the land cover coefficient x (data in Table 2), the CORINE Land Cover (2018) map with a scale of 1:650000 (Figure 3) was used.

**Figure 3.** Land cover distribution of Vjosa River Basin, Albania.

The slope map (Figure 4) of the Vjosa River Basin generated by a Digital Elevation Model (DEM) of the Albanian State Authority for Geospatial Information with a DTM cell size of 10 x 10 m was used to evaluate the mean slope of each sub-basin m (data in Table 2). The slope for each sub-basin was defined as the ratio between the difference of the extreme quotations (max-min quotes) and the length of the two extreme points under the basin. Since the slope is referred to as a percentage, the upper value is multiplied by 100.

**Figure 4.** Slope mean in percentage of Vjosa River Basin, Albania.

The mean elevation of the Vjosa River Basin is about 885 m and is derived from the elevation map of the studied area, as shown in Figure 5. The mean elevation of each sub-basin was determined from the minimum and maximum elevations' values extracted by the elevation map.

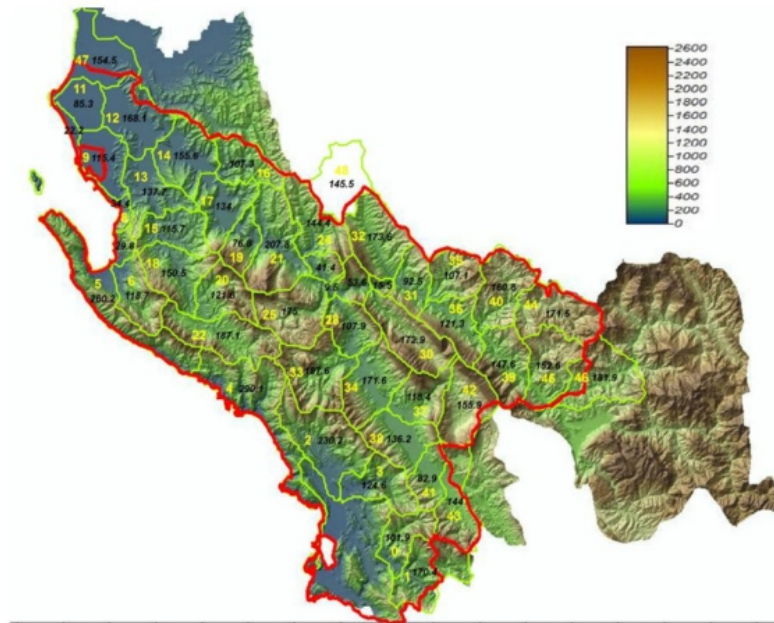


Figure 5. Elevation map of Vjosa River Basin, Albania.

Meteorological data, regarding the precipitation (h , mm) and temperature (t , °C), were obtained from 11 meteorological stations situated in the area: Brataj, Fratar Kelcyre, Krahës, Kuc, Llongo, Nivice, Permet, Polican, Selenice and Tepelene. For each meteorological station, daily temperature and precipitation data were processed to determine the mean annual value. The mean annual values of the meteorological stations are given in Table 3.

3. Results and discussion

As mentioned previously in this study, a very large dataset comprising the surface and perimeter, the coefficient of soil erodibility, land cover and mean slope and mean elevation for the sub-basins of the Vjosa River Basin was collected and used for the application of the Erosion Potential Method. Detailed information about these parameters is given in Table 2.

Table 2. Values of different parameters needed for the application of EPM in the study area.

Sub-basin	Surface (km ²)	Coef. Of soil erodibility	Land cover coefficient	Mean slope
0	101.9	0.6	0.5	25
1	170.5	0.8	0.7	20
2	230.3	0.8	0.6	15
3	124.7	0.6	0.5	18
4	290.3	0.8	0.7	22
5	260.4	0.1	0.2	28
6	118.8	0.6	0.4	17
7	29.8	0.6	0.4	15
8	34.5	0.4	0.3	15
9	115.5	0.6	0.4	5
10	22.2	0.8	0.6	2
11	85.3	0.7	0.5	2
12	168.3	0.6	0.4	4
13	137.8	0.4	0.3	8
14	155.8	0.6	0.4	10
15	115.8	0.6	0.4	13
16	107.4	0.5	0.3	12
17	134.1	0.7	0.4	14
18	150.6	0.4	0.3	12
19	76.9	0.4	0.3	20
20	121.6	0.4	0.3	24
21	207.9	0.6	0.4	14
22	187.2	0.7	0.5	21
23	41.5	0.6	0.4	16
24	144.5	0.5	0.3	18
25	175.1	0.4	0.3	20
26	9.5	0.4	0.3	19
27	53.6	0.7	0.4	17
28	107.9	0.5	0.3	18
29	15.6	0.5	0.3	16
30	172.9	0.8	0.6	21
31	92.5	0.3	0.3	23
32	173.7	0.3	0.3	24
33	187.7	0.6	0.4	23
34	171.7	0.9	0.5	26
35	107.1	0.5	0.3	22
36	121.4	0.4	0.3	20
37	118.4	0.8	0.6	23
38	136.2	0.8	0.6	21
39	147.6	0.7	0.3	20
40	160.9	0.4	0.2	22
41	83	0.8	0.6	24
42	156	0.4	0.4	21
43	144.1	0.7	0.6	18
44	171.5	0.4	0.2	19
45	152.7	0.4	0.4	18
46	182	0.4	0.3	18
47	154.6	0.6	0.4	2
48	145.6	0.4	0.3	22

The geology of the Vjosa Basin in Albania is part of five geotectonic zones, the largest of which is the Ionian zone. This zone is dominated by sand and gravel alluvial deposits in the river valley, formed by Neogene's deposits composed of sandstone, siltstone, conglomerate and partly marlstone, flysch deposits, karstic calcareous deposits and ultrabasic rock [35].

The mean slope of the area varies between 2 and 28%, where the steeper sub-basin slope belongs to the upper reach, while the low slope is in the lower part for the last 40 km before discharging.

The Vjosa river basin has high ecological values due to the presence of rare flora species. In Albania there is growth of different species, like rare Macedonian fir (*Abies borisii-regis*), plane trees, willows, maples, linden trees and hornbeams. Another important zone of the Vjosa river basin is where salt tolerant vegetation species grow, such as *Arthrocnemum fruticosum*, *Polypogon monspeliensis*, *Juncus acutus*, *Juncus maritimus*, *Agropyron litorale*, *Tamarix dalmatica* and *Limonium vulgare*.

The climate of the VRB is mainly characterized by mild winters with abundant precipitation and hot, dry summers. Due to the geographical position, the Vjosa River Basin covers different climate zones, including Alpine conditions, without glacials, in the higher altitudes; Mediterranean continental conditions in the highlands; and typical Mediterranean climate for the coastal area. For the 11 meteorological stations of the Vjosa River Basin (Table 3), the mean annual temperature varies from 11 to 17 °C, while for the precipitation, the mean annual values vary between 75 and 200 mm.

Table 3. Average annual temperatures and precipitations of the meteorological stations of the Vjosa River Basin.

Meteorologic station	Brataj	Fratar	Kelcyre	Krahes	Kuc	Llongo	Nivice	Permet	Polican	Selenice	Tepelene
h (mm)	190.2	83.3	114.8	75.9	195	173.2	198.4	109.8	167.7	81.2	11.4
t (°C)	16.1	15.6	15.4	16.2	13.5	14.6	12.6	14.4	11.1	17	16.8

The application of the Erosion Potential Method using all the parameters of Table 2 and 3 gave the following results: the erosion coefficient, the amount of eroded sediment, the sediment delivery ratio, the specific eroded sediment and the sediment yield of the sub-basins. Table 4 presents the results obtained for all sub-basins of the Vjosa River Basin from the calculations made according to Eqs 1 and 3 of the Erosion Potential Method. Meanwhile, the results about the specific eroded sediment were obtained as a report of eroded material and the surface of the sub-basins, expressed in ha.

Table 4. Results of the EPM for all sub-basins of the Vjosa River Basin.

Sub-basin	Erosion coefficient Z (--)	Eroded sediment W (m ³ /yr)	Specific eroded sediment E (m ³ /ha/yr)
0	0.27	86786.5	8.52
1	0.47	338242.6	19.84
2	0.38	423430.6	18.38
3	0.28	144098.7	11.56
4	0.71	583837.4	20.11
5	0.02	1866.75	0.07
6	0.19	34329.45	2.89
7	0.16	6701.8	2.25
8	0.07	2166.9	0.63
9	0.1	12568.75	1.09
10	0.26	10006.75	4.5
11	0.12	11828.65	1.39
12	0.1	16805.05	1
13	0.08	10850.55	0.79
14	0.17	37274.4	2.39
15	0.28	117918.5	10.19
16	0.11	14745.55	1.37
17	0.19	40305.7	3.01

18	0.11	39927.6	2.65
19	0.11	10799.95	1.41
20	0.13	39842	3.28
21	0.19	53987.3	2.6
22	0.44	378983.1	20.24
23	0.19	27632.4	6.66
24	0.12	20369.2	1.41
25	0.13	61734.5	3.53
26	0.12	3295.15	3.47
27	0.23	30029.05	5.6
28	0.14	28767.85	2.67
29	0.14	3996.5	2.57
30	0.46	261423.2	15.12
31	0.08	9985.8	1.08
32	0.08	20334.3	1.17
33	0.19	120224.3	6.41
34	0.5	333346	19.41
35	0.1	16503.25	1.54
36	0.09	15798.65	1.3
37	0.33	121326.8	10.25
38	0.46	233690.9	17.15
39	0.18	46965.05	3.18
40	0.05	8447.7	0.53
41	0.38	117632.9	14.18
42	0.01	43662.65	2.8
43	0.35	178184.5	12.37
44	0.05	8343.35	0.49
45	0.13	31009.1	2.03
46	0.12	33253.05	1.83
47	0.08	12173.4	0.79
48	0.1	25325.1	1.74

The erosion coefficient Z of the studied area varies between 0.01 and 0.71. The lowest value corresponds to sub-basin 42, while the highest corresponds to sub-basin 4. According to the Gavrilovic classifications, the results of Table 4 show heavy erosion (II erosion category) only for sub-basin 4 ($Z = 0.71$); medium erosion (III erosion category) for sub-basin 1 ($Z = 0.47$), sub-basins 30 and 38 ($Z = 0.46$) and sub-basin 22 ($Z = 0.44$); slight erosion (IV erosion category) for sub-basins 2, 41, 43, 37, 15, 3, 0, 10 and 27; and very slight erosion (V erosion category) for all the other sub-basins. According to these results, erosion in the Vjosa River Basin, is categorized as follows (see Figure 6): 2% heavy erosion, 8% medium erosion, 18% slight erosion and 72% very slight erosion.

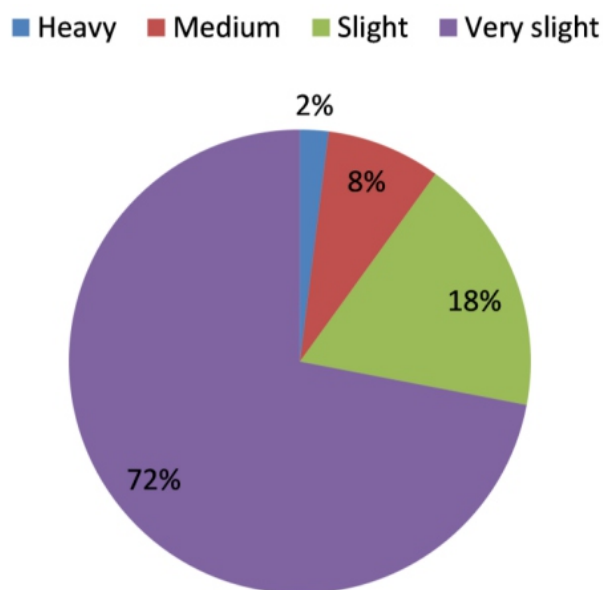


Figure 6. Soil erosion categories according the erosion coefficient Z.

As shown in Table 4, the application of EPM estimated a volume of 4230759 m³/year of eroded sediment for the Vjosa River Basin. From Table 4 and Figure 7, it is clear that the largest contribution to the annual amount of eroded sediment was given by the volume of sub-basin 4, followed by subbasins 2, 22, 1 and 34, with these respective values: 583837.4 m³/year, 423430.6 m³/year, 373883.1 m³/year, 338242.6 m³/year and 333346.0 m³/year. On the other hand, the smallest contribution to this value was given by sub-basin 5, with 1866.8 m³/year of eroded sediment, followed by sub-basin 8 with 2166.9 m³/year of eroded sediment, sub-basin 26 with 3295.2 m³/year of eroded sediment, sub-basin 29 with 3996.5 m³/year of eroded sediment and sub-basin 7 with 6701.8 m³/year of eroded sediment. All the other sub-basins have their contributions, according to the values given in Table 4, to the total amount of eroded material for the Vjosa River Basin

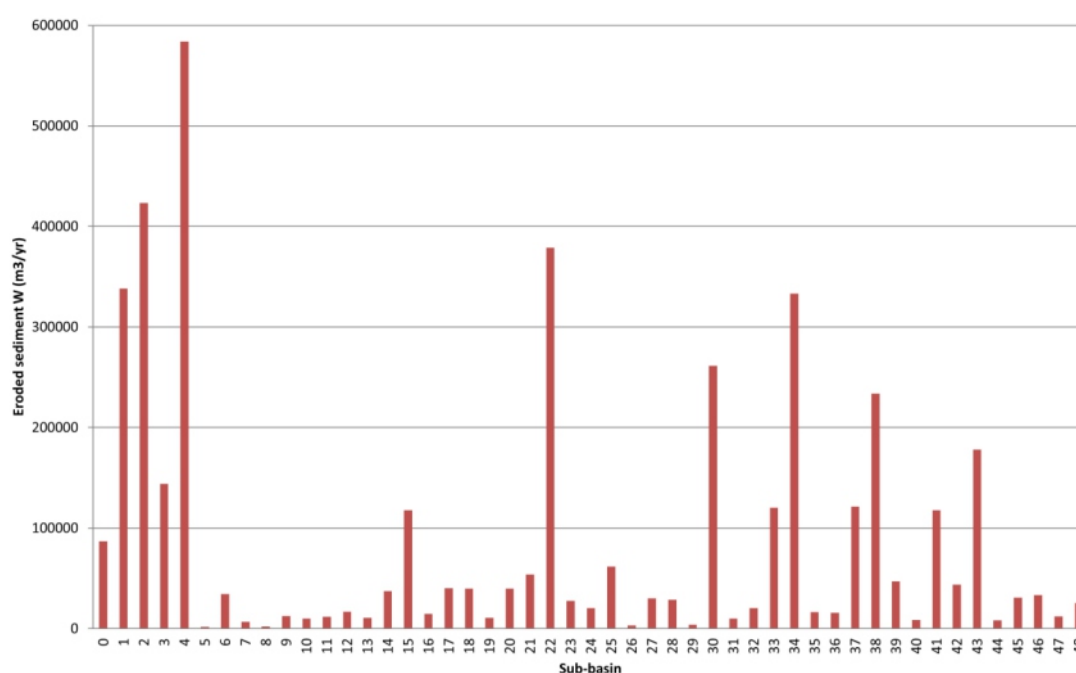


Figure 7. The quantity of eroded sediment W for each sub-basin of the Vjosa River Basin.

Based also on the equation used to calculate the eroded sediment W , the parameters which mostly affect this value are the surface S and the erosion coefficient Z . Sub-basin 4, with the largest amount of eroded material, has the highest erosion coefficient and has the biggest surface ($S = 290.3 \text{ km}^2$). According to the sensitive analyses performed by Dragicevic et al. [37], there are two parameters that affect the amount of eroded sediment W , the coefficient of soil erodibility y and the land cover coefficient x (values in Table 2). Sub-basin 4 has the highest value of land cover coefficient (0.7) but not the highest for the coefficient of soil erodibility (0.8). Sub-basin 34 has the highest value of the coefficient of soil erodibility (0.9), but the amount of eroded material is not the largest because this sub-basin has a smaller land cover coefficient and surface compared to sub-basin 4. Sub-basin 5 has the lowest value for soil erodibility (0.1) and land cover coefficient (0.2), as reflected in the result of the eroded material.

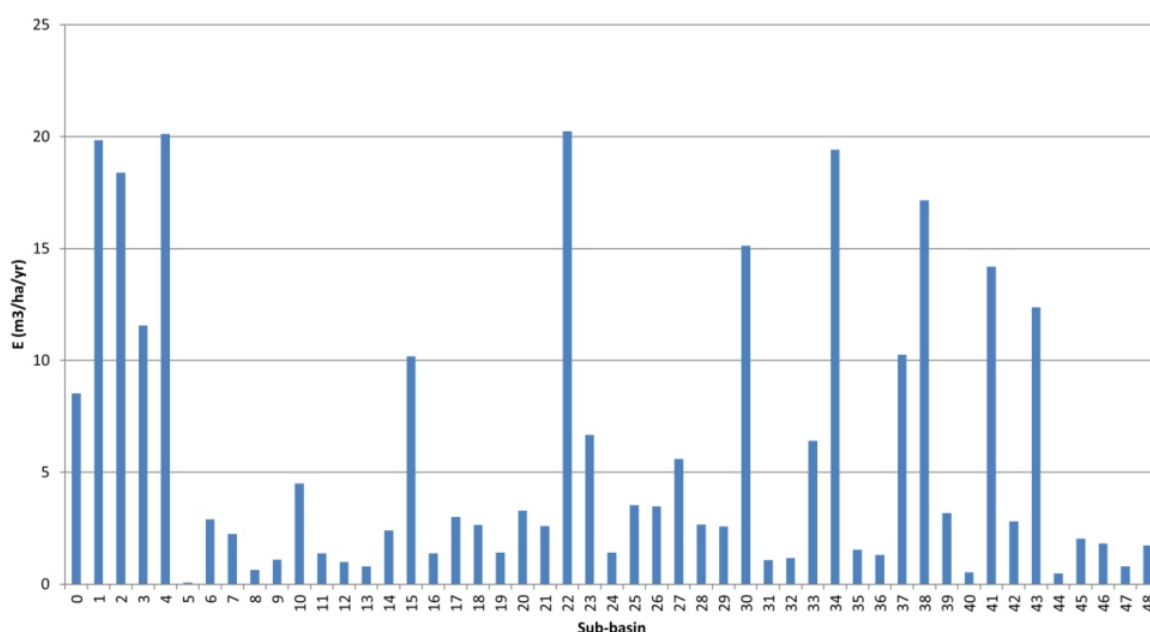


Figure 8. The quantity of specific eroded sediment E for each sub-basin of the Vjosa River Basin.

In this study we calculated also the specific eroded sediment values E . As can be seen in Table 4 and Figure 8, sub-basin 22 has the largest amount of eroded sediment per hectare per year (20.24 m³/ha/year), followed by sub-basin 4 (20.11 m³/ha/year), sub-basin 1 (19.84 m³/ha/year), sub-basin 34 (19.41 m³/ha/year) and sub-basin 2 (18.38 m³/ha/year). Sub-basin 5 has the smallest amount of eroded sediment per hectare per year (0.07 m³/ha/year). As explained previously, the specific eroded sediment is calculated as a report of the amount of eroded material and the surface of each sub-basin. It can be seen that the results for the specific eroded sediment (E) are not in the same order as those for the eroded sediment (W), due to the fact that even the surfaces of the sub-basins do not follow that order. Considering the results obtained by the calculations of specific eroded sediment (E) of the Vjosa River Basin, it is evident that the sub-basins 4 and 22 are the only sub-basins with very high erosion risk. Sub-basins 1, 2, 3, 15, 30, 34, 37, 38, 41 and 43 shows high erosion risk, while sub-basins 0, 23, 27 and 33 show moderate erosion risk, and all the other sub-basins show low or very low erosion risk. Applying Eqs 4 and 5 of the EPM, the sediment delivery ratio and sediment yield were calculated for the entire Vjosa River Basin. The results of these calculation are a delivery ratio of 0.55 and a sediment yield of 2326917

m³/year. This amount is deposited in different parts of the Vjosa River Basin, mainly in the sub-basins where the land cover coefficient, the altitude above sea level and the pronounced slopes are combined with their highest values.

4. Conclusions

In this study, the application of the Erosion Potential Method was proposed for the Vjosa River Basin, as an appropriate method for the Albanian situation. The Erosion Potential Method provides an estimate of the amount of sediment production, the erosion coefficient, the sediment yield, specific eroded sediment and the erosion intensity and risk. EPM was applied to 49 sub-basins of the Vjosa River Basin in Albania. The overall sediment production in the Vjosa River Basin is 4230759 m³/year, the mean specific eroded sediment is 6.53 m³/ha/year, and the overall real sediment production is 232917 m³/year. The major contributors in all the results obtained for the sediment production and the real sediment production are the sub-basins 1, 2, 4, 22 and 34. The erosion coefficient *Z* of each subbasin was calculated, and it varies between 0.01 (sub-basin 42) and 0.71 (sub-basin 4). According to the Gavrilovic classifications, 2% of the study area shows heavy erosion (II erosion category), with 8% medium erosion (III erosion category), 18% slight erosion (IV erosion category) and 72% very slight erosion (V erosion category).

The Erosion Potential Method is feasible for the area chosen in this study. The application of this methodology can be extended in other country areas that need to be evaluated. Information gained from the results of this study can serve to update the data regarding erosion of the Vjosa River. Further, this information can be used by the national and local authorities to establish new strategies for Vjosa River Basin protection.

Conflict of interest

The authors have no conflicts of interest to declare.

References

1. Joy TJ, Foster GR, Renard KG (2002) *Soil erosion: Processes, prediction, measurement and control*. John Wiley Sons Inc
2. Devátý J, Dostál T, Hösl R, et al. (2019) *Effects of historical land use and land pattern changes on soil erosion-Case studies from Lower Austria and Central Bohemia*. *Land Use Policy* 82: 674–685. <https://doi.org/10.1016/j.landusepol.2018.11.058>
3. Smith P, House JI, Bustamante M. et al. (2016) *Global change pressures on soils from land use and management*. *Global Change Biol* 22: 1008–1028. <https://doi.org/10.1111/gcb.13068>
4. Shojaei S, Kalantari Z, Rodrigo-Comino J (2020) *Prediction of factors affecting activation of soil erosion by mathematical modeling at pedon scale under laboratory conditions*. *Sci Rep* 10. <https://doi.org/10.1038/s41598-020-76926-1>
5. Borrelli P, Robinson DA, Panagos P, et al. (2020) *Land use and climate change impacts on global soil erosion by water (2015–2070)*. *PNAS* <https://doi.org/10.1073/pnas.2001403117>
6. Nearing MA, Pruski FF, O'neal MR (2004) *Expected climate change impacts on soil erosion rates: A review*. *J Soil Water Conserv* 59: 43–50.
7. Congo-Rwanda DR, Karamage F, Shao H, et al. (2016) *Deforestation Effects on Soil Erosion in the Lake Kivu Basin, Forests*.
8. Wenger AS, Atkinson S, Santini T, et al. (2018) *Predicting the impact of wlogging activities on soil erosion and water quality in steep, forested tropical islands*. *Environ Res Lett* 13. <https://doi.org/10.1088/1748-9326/aab9eb>

9. Zhao L, Hou R (2019) *Human causes of soil loss in rural karst environments: a case study of Guizhou, China. Sci Rep* 9: 3225. <https://doi.org/10.1038/s41598-018-35808-3>
10. Lal R (2001) *Soil degradation by erosion. Land Degrad Dev* 12: 519–539. <https://doi.org/10.1002/ldr.472>
11. Sthiannopkao S, Takizawa S, Wirojanagud W (2006) *Effects of soil erosion on water quality and water uses in the upper Phong watershed. Water Sci Technol* <https://doi.org/10.2166/wst.2006.037>
12. Acharya AK, Kafle N (2009) *Land degradation issues in Nepal and its management through agroforestry. J Agric Environ* 10: 133–143. <https://doi.org/10.3126/aej.v10i0.2138>
13. Issaka S, Ashraf MA (2017) *Impact of soil erosion and degradation on water quality: a review. Geol Ecol Landsc* <https://doi.org/10.1080/24749508.2017.1301053>
14. Chalise D, Kumar L, Kristiansen P (2019) *Land degradation by soil erosion in Nepal: A Review. Soil Systems* 3: 12. <https://doi.org/10.3390/soilsystems3010012>
15. Camara M, Jamil NR, Abdullah AFB (2019) *Impact of land uses on water quality in Malaysia: a review. Ecol Process* <https://doi.org/10.1186/s13717-019-0164-x>
16. Wischmeier WH, Smith DD (1965) *Prediction Rainfall Erosion Losses from Cropland East of the Rocky Mountains: A Guide for Selection of Practices for Soil and Water Conservation. Agr Handb* 282.
17. Kenneth GR, George RF, Glenn AW, Jeffrey PP (1991) *RUSLE: Revised universal soil loss equation. J Soil Water Conserv* 46: 30–33.
18. Williams JR (1975) *Sediment-yield prediction with Universal Equation using runoff energy factor. In: Present and Prospective Technology for Predicting Sediment Yield and Sources. US Dept Agrie* 244–252.
19. Gavrilovic Z (1988) *The use of empirical method (erosion potential method) for calculating sediment production and transportation in unstudied or torrential streams (Editor White W.R. In: International Conference on River Regime) John Wiley Sons* 411–422.
20. Emmanouloudis DA, Christou OP, Filippidis E (2003) *Quantitative estimation of degradation in the Alikamon river basin using GIS. Erosion Prediction in Ungauged Basins: Integrating Methods and Techniques (Proceedings of symposium HS01 held during IUGG2003 at Sapporo). IAHS Publ. no. 279.*
21. Haghizadeh A, Teang L, Godarzi E (2009) *Forecasting Sediment with Erosion Potential Method with Emphasis on Land Use Changes at Basin. Electronic J Geotech Engn* 14.
22. Tazioli A (2009) *Evaluation of erosion in equipped basins, preliminary results of a comparison between the Gavrilovic model and direct measurements of sediment transport. Environ Geol* 56:825–831. <https://doi.org/10.1007/s00254-007-1183-y>
23. Milanese L, Pilotti M, Clerici A (2014) *The Application of the Erosion Potential Method to Alpine Areas: Methodological Improvements and Test Case. Engin Geolr Soc Terr* https://doi.org/10.1007/978-3-319-09054-2_73
24. Milanese L, Pilotti M, Clerici A, et al. (2015) *Application of an improved version of the erosion potential method in alpine areas. Ital J Engn Geol Environ* 1.
25. Lense G, Parreiras T, Moreira R, et al (2019) *Estimates of soil losses by the erosion potential method in tropical latosols. Agri Sci* <https://doi.org/10.1590/1413-7054201943012719>
26. Marko O, Gjipalaj J, Shkodrani N (2022) *Application of the Erosion Potential Method in Vithkuqi Watersheds (Southeastern Albania). J Ecol Eng* 23: 17–24. <https://doi.org/10.12911/22998993/146131>
27. Blinkov I, Kostadinov S (2010) *Applicability of various erosion risk assessment methods for engineering purposes, BALWOIS conference, Ohrid, Macedonia.*
28. Blinkov I, Kostadinov S, Marinov I (2013) *Comparison of erosion and erosion control works in Macedonia, Serbia and Bulgaria. Int Soil Water Conserv Res* [https://doi.org/10.1016/S2095-6339\(15\)30027-7](https://doi.org/10.1016/S2095-6339(15)30027-7)

29. Vujacic D, Barovic G, Tanaskovikj V, et al. (2015) Calculation of runoff and sediment yield in the Pisevska Rijeka Watershed, Polimlje, Montenegro. *Agric For* 61: 225–234. <https://doi.org/10.17707/AgricultForest.61.2.20>
30. Spalevic V, Barovic G, Mitrovic M, et al. (2015) Assessment of sediment yield using the Erosion Potential Method (EPM) in the Karlicica watershed of Montenegro. *Conference Paper*.
31. Vujacic D, Spalevic V (2016) Assessment of Runoff and Soil Erosion in the Radulicka Rijeka Watershed, Polimlje, Montenegro. *Agric For* 62: 283–292. <https://doi.org/10.17707/AgricultForest.62.2.25>
32. Maliqi E, Sing SK (2019) Quantitative Estimation of Soil Erosion Using Open-Access Earth Observation Data Sets and Erosion Potential Model. *Water Conserv Sci Eng* 4: 187–200. <https://doi.org/10.1007/s41101-019-00078-1>
33. Gocic M, Dragicevic S, Radivojevic A, et al. (2020) Changes in Soil Erosion Intensity Caused by Land Use and Demographic Changes in the Jablanica River Basin, Serbia. *Agriculture* 10: 345. <https://doi.org/10.3390/agriculture10080345>
34. Marko O, Lako A, Çobani E (2011) Evaluation of soil erosion in the area of Kallmet Lezha District. *Geotech SP* 1474–1482. [https://doi.org/10.1061/41165\(397\)151](https://doi.org/10.1061/41165(397)151)
35. Schiemer F, Drescher A, Hauer C, et al. (2018) The Vjosa River corridor: a riverine ecosystem of Europe significance. *Acta ZooBot Austria* 155: 1–40.
36. Zemljic M (1971) Calcul du debit solide - Evaluation de la vegetation comme un des facteurs anti-erosifs. In: *International Symposium Interpraevent, Villach, Austria*.
37. Dragičević N, Karleuša B, Ožanić N (2017) Erosion Potential Method (Gavrilović Method) Sensitivity Analysis. *Soil Water Res* <https://doi.org/10.17221/27/2016-SWR>

Instructions for Authors

Essentials for Publishing in this Journal

- 1 Submitted articles should not have been previously published or be currently under consideration for publication elsewhere.
- 2 Conference papers may only be submitted if the paper has been completely re-written (taken to mean more than 50%) and the author has cleared any necessary permission with the copyright owner if it has been previously copyrighted.
- 3 All our articles are refereed through a double-blind process.
- 4 All authors must declare they have read and agreed to the content of the submitted article and must sign a declaration correspond to the originality of the article.

Submission Process

All articles for this journal must be submitted using our online submissions system. <http://enrichedpub.com/> . Please use the Submit Your Article link in the Author Service area.

Manuscript Guidelines

The instructions to authors about the article preparation for publication in the Manuscripts are submitted online, through the e-Ur (Electronic editing) system, developed by **Enriched Publications Pvt. Ltd.** The article should contain the abstract with keywords, introduction, body, conclusion, references and the summary in English language (without heading and subheading enumeration). The article length should not exceed 16 pages of A4 paper format.

Title

The title should be informative. It is in both Journal's and author's best interest to use terms suitable. For indexing and word search. If there are no such terms in the title, the author is strongly advised to add a subtitle. The title should be given in English as well. The titles precede the abstract and the summary in an appropriate language.

Letterhead Title

The letterhead title is given at a top of each page for easier identification of article copies in an Electronic form in particular. It contains the author's surname and first name initial .article title, journal title and collation (year, volume, and issue, first and last page). The journal and article titles can be given in a shortened form.

Author's Name

Full name(s) of author(s) should be used. It is advisable to give the middle initial. Names are given in their original form.

Contact Details

The postal address or the e-mail address of the author (usually of the first one if there are more Authors) is given in the footnote at the bottom of the first page.

Type of Articles

Classification of articles is a duty of the editorial staff and is of special importance. Referees and the members of the editorial staff, or section editors, can propose a category, but the editor-in-chief has the sole responsibility for their classification. Journal articles are classified as follows:

Scientific articles:

1. Original scientific paper (giving the previously unpublished results of the author's own research based on management methods).
2. Survey paper (giving an original, detailed and critical view of a research problem or an area to which the author has made a contribution visible through his self-citation);
3. Short or preliminary communication (original management paper of full format but of a smaller extent or of a preliminary character);
4. Scientific critique or forum (discussion on a particular scientific topic, based exclusively on management argumentation) and commentaries. Exceptionally, in particular areas, a scientific paper in the Journal can be in a form of a monograph or a critical edition of scientific data (historical, archival, lexicographic, bibliographic, data survey, etc.) which were unknown or hardly accessible for scientific research.

Professional articles:

1. Professional paper (contribution offering experience useful for improvement of professional practice but not necessarily based on scientific methods);
2. Informative contribution (editorial, commentary, etc.);
3. Review (of a book, software, case study, scientific event, etc.)

Language

The article should be in English. The grammar and style of the article should be of good quality. The systematized text should be without abbreviations (except standard ones). All measurements must be in SI units. The sequence of formulae is denoted in Arabic numerals in parentheses on the right-hand side.

Abstract and Summary

An abstract is a concise informative presentation of the article content for fast and accurate Evaluation of its relevance. It is both in the Editorial Office's and the author's best interest for an abstract to contain terms often used for indexing and article search. The abstract describes the purpose of the study and the methods, outlines the findings and state the conclusions. A 100- to 250-Word abstract should be placed between the title and the keywords with the body text to follow. Besides an abstract are advised to have a summary in English, at the end of the article, after the Reference list. The summary should be structured and long up to 1/10 of the article length (it is more extensive than the abstract).

Keywords

Keywords are terms or phrases showing adequately the article content for indexing and search purposes. They should be allocated heaving in mind widely accepted international sources (index, dictionary or thesaurus), such as the Web of Science keyword list for science in general. The higher their usage frequency is the better. Up to 10 keywords immediately follow the abstract and the summary, in respective languages.

Acknowledgements

The name and the number of the project or programmed within which the article was realized is given in a separate note at the bottom of the first page together with the name of the institution which financially supported the project or programmed.

Tables and Illustrations

All the captions should be in the original language as well as in English, together with the texts in illustrations if possible. Tables are typed in the same style as the text and are denoted by numerals at the top. Photographs and drawings, placed appropriately in the text, should be clear, precise and suitable for reproduction. Drawings should be created in Word or Corel.

Citation in the Text

Citation in the text must be uniform. When citing references in the text, use the reference number set in square brackets from the Reference list at the end of the article.

Footnotes

Footnotes are given at the bottom of the page with the text they refer to. They can contain less relevant details, additional explanations or used sources (e.g. scientific material, manuals). They cannot replace the cited literature.

The article should be accompanied with a cover letter with the information about the author(s): surname, middle initial, first name, and citizen personal number, rank, title, e-mail address, and affiliation address, home address including municipality, phone number in the office and at home (or a mobile phone number). The cover letter should state the type of the article and tell which illustrations are original and which are not.

Address of the Editorial Office:

Enriched Publications Pvt. Ltd.
S-9, IInd FLOOR, MLU POCKET,
MANISH ABHINAV PLAZA-II, ABOVE FEDERAL BANK,
PLOT NO-5, SECTOR -5, DWARKA, NEW DELHI, INDIA-110075,
PHONE: - + (91)-(11)-45525005

Note

[illegible]